

# Metal Ion Sensors Based on DNAzymes and Related DNA Molecules

Xiao-Bing Zhang,<sup>1,\*</sup> Rong-Mei Kong,<sup>1</sup> and Yi Lu<sup>2,\*</sup>

<sup>1</sup>State Key Laboratory for Chemo/Biosensing and Chemometrics, College of Chemistry and Chemical Engineering, Hunan University, Changsha 410082, China; email: xzbzhang@hnu.cn

<sup>2</sup>Department of Chemistry, University of Illinois at Urbana-Champaign, Urbana, Illinois 61801; email: yi-lu@illinois.edu

Annu. Rev. Anal. Chem. 2011. 4:105–28

First published online as a Review in Advance on March 1, 2011

The *Annual Review of Analytical Chemistry* is online at [anchem.annualreviews.org](http://anchem.annualreviews.org)

This article's doi:  
10.1146/annurev.anchem.111808.073617

Copyright © 2011 by Annual Reviews.  
All rights reserved

1936-1327/11/0719-0105\$20.00

\*Corresponding authors.

## Keywords

biosensors, fluorescence, colorimetry, electrochemistry, amplification, gold nanoparticles

## Abstract

Metal ion sensors are an important yet challenging field in analytical chemistry. Despite much effort, only a limited number of metal ion sensors are available for practical use because sensor design is often a trial-and-error-dependent process. DNAzyme-based sensors, in contrast, can be developed through a systematic selection that is generalizable for a wide range of metal ions. Here, we summarize recent progress in the design of DNAzyme-based fluorescent, colorimetric, and electrochemical sensors for metal ions, such as  $\text{Pb}^{2+}$ ,  $\text{Cu}^{2+}$ ,  $\text{Hg}^{2+}$ , and  $\text{UO}_2^{2+}$ . In addition, we also describe metal ion sensors based on related DNA molecules, including T-T or C-C mismatches and G-quadruplexes.

## 1. INTRODUCTION

Metal ions play beneficial or deleterious roles in biological and environmental systems. Therefore, metal ion sensors have become a hot topic in analytical chemistry. Metal ion sensors based on small, organic molecules (1); organic polymers (2); peptides (3); proteins (4); and even intact cells (5) have been reported. However, although microarrays have been developed for protein and nucleic acid detection, there are very few platforms general enough to simultaneously sense a broad range of metal ions. DNAzyme-based sensors are filling this technology gap.

At first glance, DNA might not appear to be a good choice for a metal ion-sensing platform: As a negatively charged biopolymer, DNA can bind any positively charged metal ion, making high selectivity a challenge. However, an *in vitro* selection technique (6) has been developed to obtain DNAzymes that catalyze reactions in the presence of particular metal ions. These DNAzymes are selected from a large DNA library with  $10^{14}$  to  $10^{15}$  different sequences. DNAzymes have been selected to have binding affinities and selectivities that rival those of protein antibodies, with detection limits as low as 45 pM and selectivities of more than 1 million-fold higher for their target than for other metal ions (7–9). Antibodies cannot be obtained for molecules too small to have sufficient binding repertoires (e.g., metal ions) or for molecules with poor immunogenicity or high toxicity. DNAzymes can be selected to bind essentially any oxidation state of any metal ion (7, 8). In addition, DNAzymes are also superior to antibodies for sensing applications in terms of production costs, stability, and signal transduction. As a result, DNAzyme-based sensors using many types of signal transduction mechanisms have been developed to detect a wide range of metal ions with high selectivity and sensitivity. In addition, related DNA, such as T-T or C-C mismatches and G quadruplexes, also binds metal ions, such as  $\text{Hg}^{2+}$ ,  $\text{Ag}^+$ , and  $\text{K}^+$ , respectively. In this review, we describe recent advances in all these types of functional DNA-based metal ion biosensors.

## 2. DNAZYME-BASED BIOSENSORS FOR METAL IONS

DNA has long been considered to be a strictly genetic information reservoir (10). Since the early 1990s, however, several DNA molecules known as deoxyribozymes or DNAzymes have been reported to possess catalytic activities toward specific substrates. Thus, these molecules became the newest members of the enzyme family, joining protein enzymes and ribozymes (11). As in the case of protein enzymes, most DNAzymes require certain metal ion cofactors (12). However, DNAzymes can be more convenient to use than their more well-known counterparts because they cost less to produce and are more resistant to hydrolysis. Also, unlike protein enzymes, most DNAzymes can be denatured and renatured many times without losing their binding ability or activity toward substrates. All these features make DNAzymes particularly attractive as a metal ion biosensor platform.

Over the past two decades, DNAzymes highly specific for cofactors such as  $\text{Pb}^{2+}$  (13, 14),  $\text{Cu}^{2+}$  (15, 16),  $\text{Mg}^{2+}$  (17),  $\text{Ca}^{2+}$  (18),  $\text{Zn}^{2+}$  (19),  $\text{Co}^{2+}$  (20, 21),  $\text{Mn}^{2+}$  (16, 22, 23),  $\text{UO}_2^{2+}$  (9), and  $\text{Hg}^{2+}$  (24) have been isolated through *in vitro* selection. DNAzyme-based metal ion biosensors based on various signal transduction mechanisms, including fluorescence, colorimetry, and electrochemistry, have also been developed.

### 2.1. Fluorescent DNAzyme-Based Biosensors for Metal Ions

By virtue of its high sensitivity, fast kinetics, and high spatial resolution, fluorescence is an excellent signal transduction mechanism for DNAzyme-based metal ion biosensors, whether for *in situ* applications, real-time detection in the environment, or *in vivo* imaging. Fluorimetry can easily

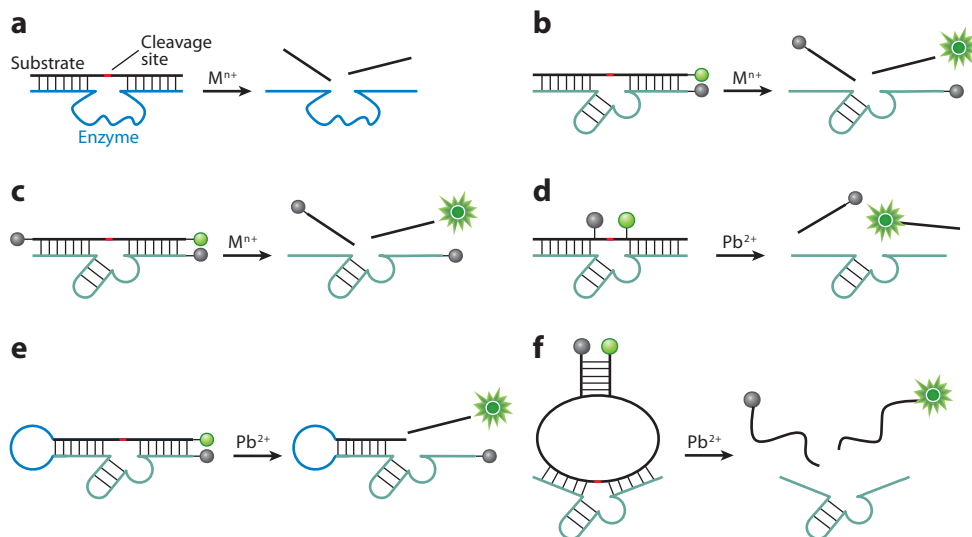


**Figure 1**

Designs of DNAzyme-based fluorescent biosensors for metal ions. (a) A typical reaction scheme for DNAzyme-based catalytic cleavage. (b–f) Various catalytic beacon designs from the literature. M denotes a generic metal ion, and  $n+$  denotes a generic number of charges.

be incorporated into DNAzyme-based cleavage reactions, such as the one shown in **Figure 1a**. The substrate strand is first hybridized with the enzyme strand. In the presence of target metal ions, the substrate cleaves into two fragments. Due to the melting temperature differences between the completely hybridized DNAzyme-substrate strand and the cleaved products, the products dissociate from the enzyme strand. When the substrate strand is functionalized with a fluorophore and the enzyme strand is functionalized with a quencher, the cleavage event leads to an increase in the fluorescent signal. In the absence of the target metal ion, the fluorophore is quenched due to the close proximity of the quencher (**Figure 1b**). When, however, the DNAzyme binds its target metal ion, it cleaves its substrate and releases the DNA fragment containing the fluorophore. Once away from the DNAzyme strand containing the quencher, the fluorophore is no longer quenched. This method is similar to molecular beacons (MBs) in that a fluorophore and a quencher are in close proximity in the absence of their target DNA or RNA but fluoresce in the presence of their target (25, 26). Because catalytic reactions are involved in the sensing process shown in **Figure 1b**, these DNAzyme-based fluorescent biosensors are termed catalytic beacons. A single target metal ion can serially bind and induce catalytic turnover in multiple DNAzyme-substrate complexes, leading to a much higher signal enhancement than from MBs. Furthermore, MBs and most other fluorescent sensors quantify analyte concentrations using fluorescence intensities. Unfortunately, this method is quite vulnerable to background fluorescence such as cellular autofluorescence. In contrast, the catalytic beacon method relates analyte concentration to the rate of changes in the fluorescent signals. This method is much more resistant to fluctuations in background fluorescence.

**2.1.1. Catalytic beacons for metal ions in a homogeneous system.** The Lu group (14) developed the first-generation fluorescent catalytic beacon based on the  $Pb^{2+}$ -dependent 8-17 DNAzyme by functionalizing the 5' end of the substrate (termed 17S) with a fluorophore and by functionalizing the 3' end of the enzyme (termed 17E) with a quencher (**Figure 1b**) (14).

In the presence of  $\text{Pb}^{2+}$  and at  $4^\circ\text{C}$ , the release of the fluorophore-labeled substrate increased the observed fluorescence by  $\sim 300\%$ . The sensor had a detection limit of  $10\text{ nM}$ , which is lower than the U.S. Environmental Protection Agency (EPA)-defined maximum contaminant level for lead in drinking water ( $72\text{ nM}$ ). However, this system showed high background fluorescence, and its performance was considerably lower at room temperature, at which the release of the fluorophore-labeled substrate produced only an  $\sim 60\%$  fluorescence increase. To solve this problem, the Lu group introduced an additional intramolecular quencher at the  $3'$  end of 17S (**Figure 1c**). This modified sensor exhibits a  $600\%$  fluorescence increase in the presence of  $6\text{ }\mu\text{M}$  of  $\text{Pb}^{2+}$  at room temperature (30), which is  $\sim 10$  times better than the performance of the first-generation sensor at room temperature. This strategy was also used to develop fluorescent catalytic beacons for other analytes, such as  $\text{UO}_2^{2+}$  (9); this sensor had a detection limit of  $45\text{ pM}$ , which rivals the detection limit of most analytical instruments. A catalytic beacon for  $\text{Cu}^{2+}$  ions was also obtained, with a detection limit of  $35\text{ nM}$  (31), lower than the  $20\text{-}\mu\text{M}$  copper maximum contaminant level defined by the EPA.

Alternatively, the Li group (32–35) employed another strategy for fluorescent catalytic biosensors by placing the fluorophore and the quencher directly adjacent to the reaction site on the substrate to achieve an even higher quenching efficiency (**Figure 1d**). This modification is not directly applicable to DNAzyme-based catalytic beacons, however, because the direct modification of the DNAzyme or substrate with bulky fluorophores or quenchers close to the cleavage site may disrupt the DNAzyme's catalytic activity. This limitation can be overcome by incorporating both a fluorophore and a quencher into the DNA pool used during *in vitro* selection (32–34).

Almost all reported DNAzyme-based fluorescent catalytic biosensors for metal ions are temperature dependent. To address this issue, the Lu group (36) proposed a novel catalytic beacon design whose performance resists temperature variations. These investigators introduced mismatches into the original DNAzyme sequence to tune its temperature stability. The resulting catalytic beacon produces the same response to its analyte at all temperatures between  $4^\circ\text{C}$  and  $30^\circ\text{C}$  (36). To date, most of the reported catalytic beacons for  $\text{Pb}^{2+}$  are based on the 8-17 DNAzyme. Although this enzyme is substantially more active in the presence of  $\text{Pb}^{2+}$  than in the presence of any other metal ion, this selectivity is not absolute: The 8-17 DNAzyme is still somewhat active in the presence of  $\text{Mg}^{2+}$ ,  $\text{Zn}^{2+}$ ,  $\text{Mn}^{2+}$ ,  $\text{Co}^{2+}$ , and  $\text{Ca}^{2+}$ . As a result, when the 8-17 DNAzyme is in solution with competing metal ions at relatively high concentrations, these metal ions can cause interference and can even reduce the effectiveness of the catalytic beacon's ability to detect  $\text{Pb}^{2+}$ . Recently, the Lu group (37) found that a classic DNAzyme (termed the GR-5 DNAzyme) selected by Breaker & Joyce (13) is more selective for  $\text{Pb}^{2+}$  than the 8-17 DNAzyme is. These researchers systematically investigated the selectivity and sensitivity of these two DNAzyme-based biosensors.  $\text{Zn}^{2+}$  showed the most active interference for both beacons, and although the 8-17 DNAzyme offers no more than a 160-fold selectivity for  $\text{Pb}^{2+}$  over  $\text{Zn}^{2+}$ , the GR-5 DNAzyme is  $\sim 40,000$  times more selective for  $\text{Pb}^{2+}$  than for  $\text{Zn}^{2+}$ .

Other groups have also designed  $\text{Pb}^{2+}$  DNAzyme-based catalytic beacons. The Tan group (38) designed a unimolecular DNA-catalytic beacon for  $\text{Pb}^{2+}$  and used it to monitor a single  $\text{Pb}^{2+}$  ion in solution by fluorescence microscopy. Instead of following the traditional catalytic beacon design (**Figure 1e**), the Tan group linked the fluorophore-labeled 17S to the quencher-labeled 17E using several thymines. This design brought the quencher into close proximity to the fluorophore in the inactive state and improved the catalytic beacon's sensitivity to  $\text{Pb}^{2+}$ . The beacon detected  $\text{Pb}^{2+}$  within a large dynamic range of nanomolar concentration, with a detection limit of  $3\text{ nM}$ .

In both first- and second-generation catalytic beacons, the DNAzyme strand was labeled with a quencher. This quencher reduced the background fluorescence. In addition, in both catalytic

beacon designs, the substrate-to-DNAzyme ratio was limited to  $\leq 1$ , making it impossible to take advantage of DNAzymes' ability to amplify fluorescent signals through multiple-turnover reactions. To realize the true multiple-turnover catalytic ability of DNAzymes for amplified sensing, the Zhang and Lu groups (39) developed a novel catalytic and molecular beacon (CAMB) for the amplified sensing of  $\text{Pb}^{2+}$  and adenosine by taking advantage of the MBs' high quenching efficiency and the catalytic beacons' multiple enzymatic turnover properties (39). In these researchers' design, the substrate strand was converted into a MB by extending the original DNAzyme substrate strand at both ends (**Figure 1f**). In the presence of  $\text{Pb}^{2+}$ , the MB substrate was cleaved into two DNA fragments, releasing the fluorophore-quencher pair from one another and thus dramatically increasing the fluorescent signal. The CAMB DNAzyme sensor was highly sensitive to  $\text{Pb}^{2+}$ : Its detection limit was 600 pM.

All the catalytic beacons discussed above require the covalent linkage of a fluorophore and quencher to DNA to produce an efficient fluorescent switch controlled by a DNA-target interaction. These labels lead to high production costs, require complex operation procedures, and potentially decrease the activity of the DNAzymes to which the labels are conjugated. Alternatively, label-free fluorescence methods may overcome these disadvantages and may improve the performance of the biosensors. To evaluate this potential, the Lu group (40) developed a label-free fluorescent catalytic sensor for  $\text{Pb}^{2+}$  by incorporating an abasic site termed dSpacer into the duplex region of the 8-17 DNAzyme. dSpacer binds 2-amino-5,6,7-trimethyl-1,8-naphthyridine (ATMND) (an extrinsic fluorescent compound) and quenches its fluorescence. When the modified 8-17 DNAzyme-based catalytic beacon was exposed to  $\text{Pb}^{2+}$ , the DNAzyme cleaved the substrate, released ATMND from the DNA duplex, and enhanced the fluorescence of ATMND. The label-free catalytic beacon's detection limit for  $\text{Pb}^{2+}$  was 4 nM, which was even lower than that of the corresponding labeled DNAzyme sensor. However, this label-free strategy does not completely avoid production costs and complications because it calls for an abasic site in the DNA strand. More recently, the same research group reported a label-free fluorescent DNAzyme sensor for  $\text{Pb}^{2+}$  that uses unmodified DNA. This sensor operates via a vacant site approach and shows a satisfying sensitivity and selectivity for  $\text{Pb}^{2+}$ , with a detection limit of 8 nM (41).

**2.1.2. DNAzyme-based fluorescent surface sensors for metal ions.** The catalytic beacons discussed above operate in the solution phase. Surface immobilization provides an alternative strategy for sensor design. For practical fluorescence applications, a surface sensor is more favorable than a solution-based sensor. First, the surface-based sensor is more amenable to washing, which can eliminate background fluorescence from cleavage products or adventitiously bound fluorescent molecules. Washing the sensor surface before detection is carried out can lower the background fluorescence significantly, which in turn can lower the detection limit. Second, reversible switches of the fluorescent signal between off (quenching) and on (enhancement) states are technically easier to achieve with the surface-based sensor, which makes the sensor reusable. Third, surface immobilization can help to stabilize DNAzyme sensors for long-term storage.

In a collaboration between the Bohn, Lu, and Sweedler groups (42), 5'-thiolated 8-17 DNAzyme was immobilized onto a gold surface to produce a fluorescent surface sensor for  $\text{Pb}^{2+}$ . These groups' experimental results indicated that, in comparison with catalytic beacons carried out in solution phase, DNAzyme-based surface sensors have lower detection limits (from 10 to 1 nM) with equivalent catalytic activities and specificities; they are also easily regenerated and stable even after long-term storage. These researchers further incorporated the 8-17 DNAzyme into gold-coated nanocapillary array membranes to build a ratiometric fluorescent sensor for  $\text{Pb}^{2+}$  using an internal standard. This sensor was active even after being stored in a prepared state for 30 days at room temperature (43). Subsequently, these investigators reported their systematic investigation

of the factors affecting the DNazymes' performance when the DNazymes were immobilized onto gold-coated nanocapillary array membranes (44). In a related work, the 8-17 DNzyme was also immobilized onto multiwalled carbon nanotubes and maintained its high catalytic activity and stability (45).

**2.1.3. Microfluidics-based catalytic beacons for metal ions.** Over the past decade, microfluidic lab-on-a-chip systems have elicited an increasing degree of interest (46, 47), as these systems reduce the consumption of expensive reagents, reduce the quantity of waste produced, allow for the precise manipulation of volumes as low as a few picoliters, can handle fast chemical reactions, allow for batch fabrication, and result in low manufacturing costs. Microfluidics are also promising platforms for miniaturized DNzyme-based biosensors for metal ions. In one example, a  $\text{Pb}^{2+}$ -specific DNzyme was introduced into a picoliter-scaled mixing subsystem on the microfluidic breadboard. This DNzyme-based biosensor can detect  $\text{Pb}^{2+}$  at concentrations as low as 500 nM in <1 nl of solution (48). By combination of the  $\text{Pb}^{2+}$ -specific 8-17 DNzyme with a microfluidic device containing two perpendicular channels interfaced by a nanocapillary array interconnect, a miniaturized lead sensor was developed. The detection limit for  $\text{Pb}^{2+}$  of this voltage-controlled device is 11 nM (49).

This DNzyme was also immobilized within a microfluidic platform for real-time  $\text{Pb}^{2+}$  detection. The DNzyme was immobilized onto the walls of a PMMA (polymethylmethacrylate) microfluidic device using the highly specific biotin-streptavidin interaction. The immobilized DNzyme retained its  $\text{Pb}^{2+}$ -dependent activity in the microfluidic device, permitted sensor regeneration and reuse, and allowed the detection zone to be localized (50). This sensor system may allow for the remote, long-term monitoring of metal ions in many environmental and medical applications.

## 2.2. Colorimetric DNzyme Biosensors for Metal Ions

Colorimetric sensors have received considerable attention in chemical and biological analysis because of their simplicity, high sensitivity, and low cost. Moreover, colorimetric sensors may minimize or even eliminate the use of analytical instruments and can easily realize on-site detection.

**2.2.1. Gold nanoparticles as color reporters for colorimetric biosensors.** Nanoparticles made of noble metals such as gold and silver possess unique size- and distance-dependent optical properties. They also exhibit very high extinction coefficients and are therefore ideal candidates for incorporation into colorimetric sensors (51). Liu & Lu (52) first reported a colorimetric DNzyme-based biosensor for  $\text{Pb}^{2+}$  that used DNA-functionalized gold nanoparticles (AuNPs) (Figure 2a). The substrate strand of the 8-17 DNzyme was extended on both ends to allow it to hybridize with DNA-functionalized AuNPs in a head-to-tail manner; the resulting AuNP aggregates appeared blue. Upon heating of the system to 50°C, the AuNPs and DNzyme disassembled, producing a red color. In the absence of  $\text{Pb}^{2+}$ , the AuNPs and DNzyme assembly were reformed by the subsequent cooling process. However,  $\text{Pb}^{2+}$  induced the cleavage of the substrate and inhibited the complex's reassembly, resulting in a permanent red color. A detection limit of 100 nM was achieved, and the sensor could detect  $\text{Pb}^{2+}$  in paint. Moreover, the sensor's dynamic range could be tuned by varying the ratio of active DNzymes to inactive mutant DNzymes.

Because the high steric effects of the head-to-tail system in this design required an annealing step to aggregate the AuNPs, the design was improved by changing the alignment to a tail-to-tail arrangement. This design allowed the AuNPs aggregates to form at room temperature (Figure 2b) (53). The Lu group (53) found that the AuNP size could affect the assembly kinetics



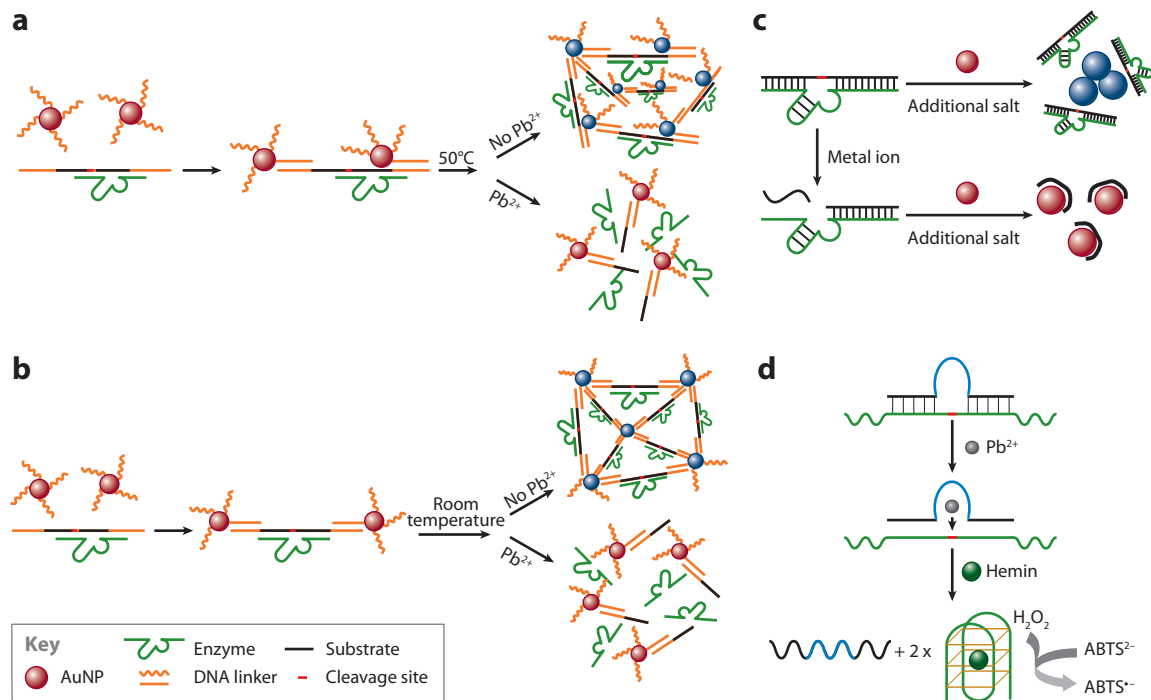


**Figure 2**

Colorimetric DNAzyme biosensors for metal ions. (a)  $Pb^{2+}$ -directed assembly of DNAzyme-linked gold nanoparticles (AuNPs) aligned in a head-to-tail manner. (b)  $Pb^{2+}$ -directed assembly of DNAzyme-linked AuNPs aligned in a tail-to-tail manner. (c) Label-free colorimetric metal ion sensors based on DNAzymes and AuNPs. (d) Analysis of  $Pb^{2+}$  by a horseradish peroxidase-mimicking DNAzyme cascade. Addition of  $Pb^{2+}$  cleaves the green substrate into two identical pieces (2x) that form G-quadruplex containing the HRP-mimicking DNAzyme sequence.  $ABTS^{2-}$ , 2,2'-azino-bis(3-ethylbenzothiazoline-6-sulfonic acid).  $ABTS^{\cdot-}$  is a radical form of  $ABTS^{2-}$ .

of the sensing system, and a distinct color change occurred in 5 min by the use of larger (42-nm) AuNPs. The above sensing systems are light-down sensors, as no color change is observed in the presence of  $Pb^{2+}$ . Lu and colleagues (54–56) further developed light-up colorimetric DNAzyme sensors for  $Pb^{2+}$  and  $UO_2^{2+}$  via the stimuli-responsive disassembly of nanoparticle aggregates. In addition to the above cleavage-dependent, disassembly-based biosensors, Liu & Lu (57) used a ligation DNAzyme to develop an assembly-based sensing system. This system was highly selective for and sensitive to  $Cu^{2+}$ .

Moving beyond biosensors requiring the induced disassembly or assembly of AuNPs, the Li group (58) developed a new type of colorimetric DNAzyme biosensor for  $Pb^{2+}$  on the basis of non-cross-linking DNA AuNP conjugates. They immobilized AuNPs with a moderate number of short, thiolated DNAzyme substrate strands and then hybridized the 8-17 DNAzyme to them. The addition of  $Pb^{2+}$  triggered the enzymatic cleavage and release of substrate strands from the AuNPs, decreased the salt stability of the AuNPs, and finally produced a red-to-purple color change due to the decrease in the number of DNA strands on the nanoparticle surface.

All the colorimetric sensors described above were based on DNA-functionalized AuNPs, which required chemically modified DNA and surface-modified AuNPs. Because the DNAzyme's cleavage of the substrate releases short single-stranded DNA (ssDNA) fragments, label-free colorimetric DNAzyme sensors based on the protection effects of nonthiolated short ssDNA for AuNPs

were also developed for  $\text{Pb}^{2+}$  and  $\text{UO}_2^{2+}$  (**Figure 2c**) (56, 59). Such label-free sensors were highly sensitive to their target metal ions, and detection limits of 3 nM for  $\text{Pb}^{2+}$  and 1 nM for  $\text{UO}_2^{2+}$  were observed. The Dong and Wang group (60) also developed a label-free colorimetric DNAzyme sensor for  $\text{Pb}^{2+}$  on the basis of a similar design.

Although the above-mentioned colorimetric biosensors represent significant progress toward real-time sensing without any need for analytical instruments, they still require laboratory techniques, such as the precise transferring and mixing of multiple solutions. These requirements make the sensors difficult for the public to use. In contrast, the lateral flow device is an ideal platform for making easy-to-use biosensors for metal ions. By immobilizing non-cross-linked nanoparticle-DNAzyme conjugates on lateral flow devices, the Lu group (61) developed an easy-to-use dipstick test for  $\text{Pb}^{2+}$  analysis. This device had a detection limit of 0.5  $\mu\text{M}$  and did not require any instrumentation. It was used to detect  $\text{Pb}^{2+}$  extracted from paints, with promising results (61).

### 2.2.2. Horseradish peroxidase-mimicking DNAzyme as a color reporter for colorimetric biosensors.

Other colorimetric agents are available in addition to metal nanoparticle-based colorimetric reporters. For example, the horseradish peroxidase (HRP)-mimicking DNAzyme shows peroxidase-like activity when hemin is present as a cofactor; HRP can effectively catalyze the  $\text{H}_2\text{O}_2$ -mediated oxidation of 2,2'-azino-bis(3-ethylbenzothiazoline-6-sulfonic acid) (ABTS, a classic substrate of peroxidase) into its radical form ( $\text{ABTS}^{\cdot-}$ ) with an obvious color change. HRP-mimicking DNAzyme was employed as an amplifying color reporter to design colorimetric DNAzyme biosensors for metal ions. By introducing the HRP-mimicking DNAzyme sequence into the substrate strand of the 8-17 DNAzyme, Willner and coworkers (62) developed a DNAzyme cascade for the amplified detection of  $\text{Pb}^{2+}$  (**Figure 2d**). In the absence of  $\text{Pb}^{2+}$ , the HRP-mimicking DNAzyme sequence hybridized to the enzyme strand and inhibited its activity. The addition of  $\text{Pb}^{2+}$  induced the cleavage of the substrate strand and liberated the activated HRP-mimicking DNAzyme, which catalyzed the oxidation of the enzyme's substrates and enabled the colorimetric or chemiluminescent detection of  $\text{Pb}^{2+}$ . Subsequently, on the basis of a similar strategy, these researchers reported a  $\text{UO}_2^{2+}$ -dependent DNAzyme cascade for the amplified colorimetric detection of  $\text{UO}_2^{2+}$  with a detection limit of 1 nM (63). By fusing a DNA-cleaving DNAzyme to an HRP-mimicking DNAzyme in one DNA molecule, Ye and coworkers (64) reported an allosteric unimolecular probe to detect  $\text{Cu}^{2+}$  colorimetrically.  $\text{Cu}^{2+}$  induced the DNA-cleaving DNAzyme to cleave its substrate, which allosterically transformed and activated the HRP-mimicking DNAzyme. The active HRP-mimicking DNAzyme catalyzed 3,3',5,5'-tetramethylbenzidine (TMB)'s reaction, which gave rise to a colorimetric signal.

## 2.3. Electrochemical DNAzyme Biosensors for Metal Ions

Due to their remarkable characteristics, such as high sensitivity, simple instrumentation, low production cost, and promising response speed, electrochemical methods have been employed to design DNAzyme-based biosensors for metal ions. Plaxco and coworkers (65) reported a DNAzyme-based electrochemical biosensor for  $\text{Pb}^{2+}$  detection (**Figure 3a**). A DNAzyme strand was functionalized with the redox-active compound methylene blue and immobilized on a gold electrode via a thiol-gold interaction. The DNAzyme was then hybridized to its substrate strand, which prohibited any contact between methylene blue and the electrode. In the presence of  $\text{Pb}^{2+}$ , the substrate was cleaved and released. Such release made the enzyme strand more flexible



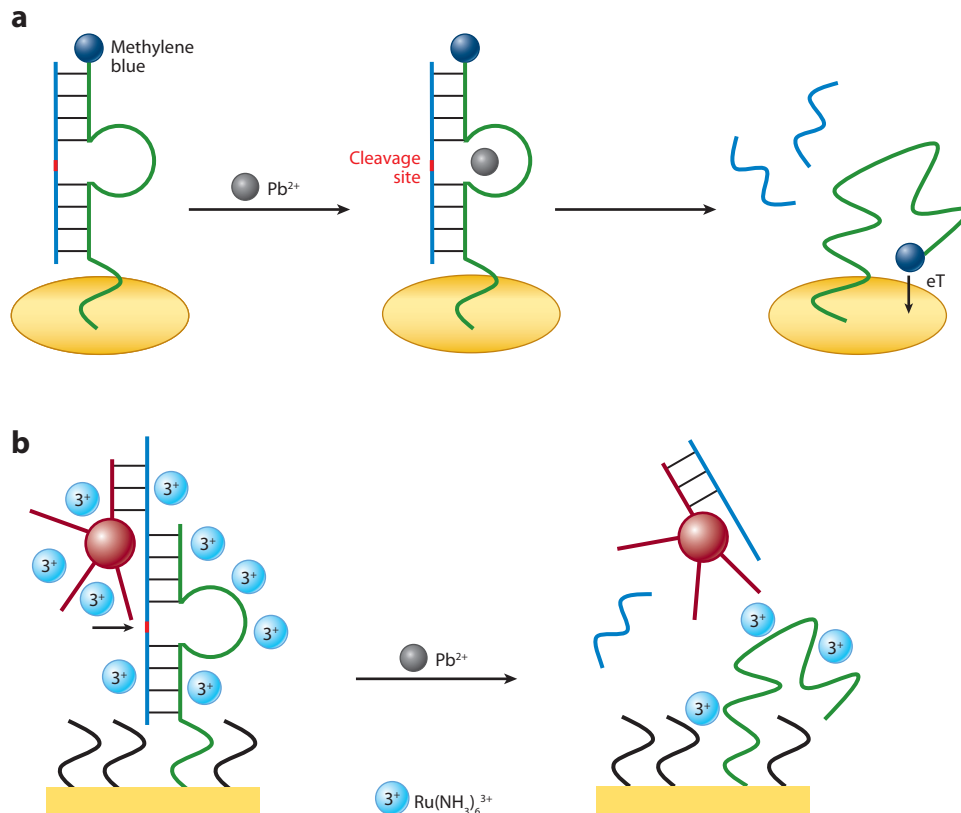


**Figure 3**

Electrochemical DNAzyme biosensors for metal ions. (a) Schematic of an electrochemical  $\text{Pb}^{2+}$  sensor based on the conformational change of a DNAzyme. eT denotes electron transfer from methylene blue to the electrode surface. (b) Schematic of a label-free electrochemical  $\text{Pb}^{2+}$  sensor with gold nanoparticle-functionalized reporter DNA as a signal amplifier.

and facilitated the electrochemical communication between the redox label and the electrode, producing an electrochemical signal proportional to the concentration of  $\text{Pb}^{2+}$  present. The biosensor had a detection limit of 300 nM and was successfully used to detect  $\text{Pb}^{2+}$  in soil samples. Shao and coworkers (66) employed reporter DNA functionalized with AuNPs to improve the sensitivity and to amplify the electrochemical signal of a DNAzyme biosensor, resulting in a detection limit of 1 nM (**Figure 3b**). A redox mediator,  $\text{Ru}(\text{NH}_3)_6^{3+}$ , which could bind to the anionic phosphate of DNA through electrostatic interactions, was chosen as the electrochemical signal transducer (66). Recently, Tian and coworkers (67) proposed a novel assembly strategy to develop an electrochemical DNAzyme biosensor for the amplified detection of  $\text{Pb}^{2+}$ . They modified 17E with AuNPs and hybridized it to 17S, whereas a capture DNA strand was immobilized onto the surface of the gold electrode. In the presence of  $\text{Pb}^{2+}$ , the substrate was cleaved and released from the enzyme, and free 17E on the AuNPs hybridized with the capture DNA on the gold electrode, resulting in an enhanced electrochemical signal. The high signal amplification coupled with the low background noise led to a detection limit of 0.028 nM for  $\text{Pb}^{2+}$ .

### 3. BIOSENSORS BASED ON METAL ION-STABILIZED DNA MISMATCHES

Metal ions such as  $\text{Hg}^{2+}$  and  $\text{Ag}^+$  can selectively bind certain DNA bases to form strong metal-base complexes. Such complexes can, in turn, stabilize DNA mismatches in the DNA duplex (68, 69). On the basis of this phenomenon, various signal transduction mechanisms, including fluorescence, colorimetry, and electrochemistry, have been employed to develop DNA mismatch-based biosensors for  $\text{Hg}^{2+}$  and  $\text{Ag}^+$ .

#### 3.1. T-T Mismatch-Based Biosensors for $\text{Hg}^{2+}$

Ono & Togashi (68) first reported that  $\text{Hg}^{2+}$  can specifically bind to two DNA thymine (T) bases, can form strong T- $\text{Hg}^{2+}$ -T pairs in a DNA duplex, and can thermally stabilize the DNA duplex. These investigators also probed the chemical structure of the T- $\text{Hg}^{2+}$ -T pair with  $^1\text{H}$  NMR (nuclear magnetic resonance) and  $^{15}\text{N}$  NMR spectroscopy (70, 71). T- $\text{Hg}^{2+}$ -T coordination chemistry was then adopted to construct biosensors for  $\text{Hg}^{2+}$  on the basis of various signal transduction mechanisms.

**3.1.1. T- $\text{Hg}^{2+}$ -T-based fluorescent biosensors for  $\text{Hg}^{2+}$ .** Ono & Togashi (68) were the first to design a fluorescent, T-T mismatch-based biosensor. A T-rich DNA strand was functionalized with a fluorophore and a quencher on its 3' terminus and its 5' terminus, respectively (**Figure 4a**).  $\text{Hg}^{2+}$  induced the T- $\text{Hg}^{2+}$ -T base pair to form, bringing the two ends of the DNA probe close to each other and quenching the fluorescent emission. The sensor had a detection limit of 40 nM for  $\text{Hg}^{2+}$ . Chen and coworkers (72) found that  $\text{Hg}^{2+}$  can quench the fluorescence of a single, fluorophore-labeled oligodeoxyribonucleotide containing consecutive Ts via photoinduced charge transfer between the fluorophore and  $\pi$ -stacked T- $\text{Hg}^{2+}$ -T base pairs. On the basis of this finding, they designed a fluorescent biosensor for  $\text{Hg}^{2+}$  with a detection limit of 20 nM (72). However, the turn-off characteristic of these biosensors made them prone to false positives from quenchers in environmental or clinical samples. By introducing T-T mismatches in the stem region of the uranium-specific DNAzyme, Liu & Lu (73) reported a catalytic DNA biosensor for the turn-on detection of  $\text{Hg}^{2+}$  that amplified its signal through allosteric interactions, resulting in a detection limit of 2.4 nM. However, this method required the use of toxic uranium ions as cofactors. To overcome this drawback, Wang et al. (74) developed a structure-switching-based fluorescent turn-on sensor for  $\text{Hg}^{2+}$ . This sensor had a detection limit of 3.2 nM (**Figure 4b**) and

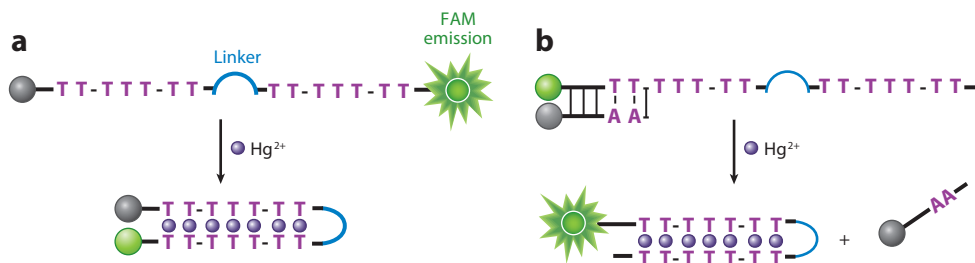


**Figure 4**

Thymine (T)- $\text{Hg}^{2+}$ -T-based fluorescent sensors covalently modified with fluorophores. (a) Schematic of a turn-off fluorescent sensor.  $\text{Hg}^{2+}$  mediates T- $\text{Hg}^{2+}$ -T base pair formation and induces a hairpin structure to form. (b) Schematic of a turn-on fluorescent mercury sensor based on a structure-switching strategy.

was successfully used to detect  $\text{Hg}^{2+}$  in pond water. Using AuNPs' excellent quenching properties, Yang and coworkers (75) employed a new T-T mismatch-based design to detect  $\text{Hg}^{2+}$  visually or fluorescently in aqueous solution. Similar to AuNPs, single-walled carbon nanotubes (SWCNTs) also have excellent quenching properties. The Wang group (76) developed a fluorescent biosensor based on T-rich DNA and SWCNTs to detect  $\text{Hg}^{2+}$  at concentrations as low as 14.5 nM.

In addition to fluorescent biosensors based on emission intensity changes, Ye and coworkers (77) reported a fluorescence polarization assay-based T-T mismatch biosensor to detect  $\text{Hg}^{2+}$ . By use of an AuNP-enhancement approach, the sensor achieved a detection limit as low as 1.0 nM.

The T-T mismatch-based biosensors described above require the DNA to be functionalized with fluorophores. Alternatively, DNA-intercalating dyes such as TOTO-3 and SYBR Green I, as well as the molecular light-switch complex  $[\text{Ru}(\text{phen})_2(\text{dppz})]^{2+}$ , have been employed in the design of label-free T- $\text{Hg}^{2+}$ -T-based fluorescent biosensors. Binding of these dyes to double-stranded DNA (dsDNA) strongly enhances their fluorescence. Chang and coworkers (78) mixed TOTO-3 with a poly-T oligonucleotide and studied their fluorescence properties in the presence and absence of  $\text{Hg}^{2+}$ . The addition of  $\text{Hg}^{2+}$  induced the poly-T oligonucleotide to fold into a dsDNA structure, enhancing the fluorescence intensity of TOTO-3. Several groups employed SYBR Green I as a fluorescent reporter in different label-free designs based on T- $\text{Hg}^{2+}$ -T (79–81). The Chang group (82) developed a fluorescent biosensor for  $\text{Hg}^{2+}$  using T-rich DNA-functionalized AuNPs as a recognition unit and OliGreen as a fluorescent reporter. In the presence of  $\text{Hg}^{2+}$ , the formation of T- $\text{Hg}^{2+}$ -T base pairs induced the DNA on AuNPs to form hairpin structures. This, in turn, released some DNA molecules from the surface of the AuNPs into the bulk solution, where the DNA reacted with OliGreen. The fluorescence of the OliGreen-DNA complexes increased with  $\text{Hg}^{2+}$  concentration, and  $\text{Hg}^{2+}$  was detected at concentrations as low as 25 nM. Kumar & Zhang (83) labeled photon-upconverting  $\text{NaYF}_4:\text{Yb}^{3+}, \text{Tm}^{3+}$  nanoparticles with T-rich ssDNA to form a fluorescence resonance energy transfer (FRET)-based biosensor for  $\text{Hg}^{2+}$  with SYBR Green I as an acceptor. The addition of  $\text{Hg}^{2+}$  induced the folding of the T-rich ssDNA and initiated the FRET process between photon-upconverting nanoparticles and SYBR Green I. Zhang and coworkers (84) also employed the metal complex  $[\text{Ru}(\text{phen})_2(\text{dppz})]^{2+}$  as a fluorescent reporter in a label-free biosensor for  $\text{Hg}^{2+}$ . The luminescence of  $[\text{Ru}(\text{phen})_2(\text{dppz})]^{2+}$  was very weak in aqueous solution, and significant fluorescence enhancement was observed after the Ru complex intercalated  $\text{Hg}^{2+}$ -stabilized DNA duplexes. This sensing system had a detection limit of 0.35 nM.

In addition to DNA-intercalating dyes, cationic conjugated polymers have also been used in fluorescent biosensors due to their excellent optical and electronic properties. Fan and coworkers (85) employed a water-soluble, cation-conjugated polymer and a T-rich DNA probe to develop a turn-on, label-free fluorescent  $\text{Hg}^{2+}$  biosensor. In the absence of  $\text{Hg}^{2+}$ , the cation-conjugated polymer and the random coil-like DNA probe formed an electrostatic complex with a characteristic red color and a weak fluorescence. Upon addition of  $\text{Hg}^{2+}$ , a color change from red to yellow accompanied by a significant fluorescence enhancement were observed. The biosensor provided micromolar sensitivity to  $\text{Hg}^{2+}$  when using the naked eye, and nanomolar sensitivity was achieved by fluorimetry. Ren & Xu (86) reported a cation-conjugated polymer-based FRET biosensor for  $\text{Hg}^{2+}$  using a poly-T oligonucleotide as a  $\text{Hg}^{2+}$  ligand and YOYO-1 as an acceptor. In the presence of  $\text{Hg}^{2+}$ , the polymer wrapped around the folded poly-T oligonucleotide- $\text{Hg}^{2+}$ -YOYO-1 complex. FRET occurred between the polymer and YOYO-1, amplifying the signal and producing a detection limit of 3.2 nM. Wang & Liu (87) built upon this design, adding in AuNPs. They reported a T-T mismatch-based fluorescence turn-on sensor system for the amplified detection of  $\text{Hg}^{2+}$  at concentrations as low as 5 nM.

**3.1.2. T-T mismatch-based colorimetric biosensors for  $\text{Hg}^{2+}$ .** Beyond fluorescent biosensors, T-T mismatch-based colorimetric biosensors have also attracted increasing interest in recent years. Mirkin and coworkers (88) reported a colorimetric  $\text{Hg}^{2+}$  sensor based on T- $\text{Hg}^{2+}$ -T coordination chemistry. Beginning with two complementary, T-T mismatch-containing ssDNAs on different AuNPs,  $\text{Hg}^{2+}$  stabilized the hybridization of the two DNA strands, forming AuNP aggregates that were more thermally stable. The concentration of  $\text{Hg}^{2+}$  was determined by monitoring the change in the solution color at the melting temperature of the DNA-AuNP aggregates. This method had a detection limit of 100 nM. The need for a temperature control unit made this system unfavorable for rapid, on-site assays. By significantly improving the sensor design, Liu and coworkers (89) employed DNA-AuNP conjugates and T- $\text{Hg}^{2+}$ -T coordination chemistry to develop a sensor system that worked at ambient temperature and that rapidly detected mercury in a single step at concentrations as low as 1  $\mu\text{M}$ .

The colorimetric biosensors for  $\text{Hg}^{2+}$  discussed above were based on the aggregation of cross-linking DNA-AuNPs. Song and coworkers (90) developed a non-cross-linking DNA-AuNP-based  $\text{Hg}^{2+}$  biosensor with the help of a power-free poly(dimethylsiloxane) microfluidic device at room temperature. A thiolated, T-rich ssDNA was immobilized onto the surface of an AuNP. In the presence of  $\text{Hg}^{2+}$ , adjacent T probes at the surface of each AuNP formed T- $\text{Hg}^{2+}$ -T complexes. This in turn changed the charge distribution at the surface and destabilized the AuNPs, causing the solution to turn purple.

ssDNA's protective effects on AuNPs were also applied to build label-free colorimetric biosensors for  $\text{Hg}^{2+}$ . By using AuNPs and T-rich ssDNA, the Willner group (91) reported a label-free colorimetric  $\text{Hg}^{2+}$  biosensor with a detection limit of 10 nM. In the presence of  $\text{Hg}^{2+}$ , the formation of T- $\text{Hg}^{2+}$ -T complexes yielded a hairpin complex that desorbed the ssDNA from the AuNPs. The AuNPs then aggregated, causing the color of the solution to change from red to blue (91). On the basis of a similar principle, a series of label-free colorimetric sensors for the sensitive and selective detection of  $\text{Hg}^{2+}$  were further reported (92–94).

In addition to metal nanoparticles, an HRP-mimicking DNzyme was also employed as an amplifying colorimetric reporter to design T- $\text{Hg}^{2+}$ -T-based colorimetric biosensors. The Willner group (91) used this DNzyme to build a DNA-based molecular machine to detect  $\text{Hg}^{2+}$ . With two amplification steps involved, this sensor system showed a detection limit of 1.0 nM for  $\text{Hg}^{2+}$  (91). By utilizing a  $\text{Hg}^{2+}$ -mediated T-T mismatch pair to modulate the proper folding of G-quadruplex DNA and to inhibit the DNzyme's activity, Wang and coworkers (95) developed a label-free colorimetric biosensor for  $\text{Hg}^{2+}$  with a detection limit of 50 nM. Wang and coworkers further reported a human telomeric DNA-based colorimetric sensor for  $\text{Hg}^{2+}$  detection using TMB as a substrate (96). On the basis of a similar design, Zhong and coworkers (97) developed a T-rich G-quadruplex DNA-based colorimetric  $\text{Hg}^{2+}$  biosensor and employed a blotting membrane as the detection platform to improve the sensitivity. This method enabled  $\text{Hg}^{2+}$  at concentrations as low as 0.1 nM to be detected with the aid of a scanner. By integrating a T-rich sequence for  $\text{Hg}^{2+}$  recognition and two flanking G-quadruplex halves for allosteric signal transductions, Deng and coworkers (98) developed a label-free colorimetric biosensor for  $\text{Hg}^{2+}$  with a detection limit of 4.5 nM. Recently, Kong and coworkers (99) reported that the addition of  $\text{Hg}^{2+}$  can enhance the catalytic activity of  $\text{T}_4\text{G}_3$ -hemin complexes; this finding was applied to develop a label-free colorimetric biosensor for  $\text{Hg}^{2+}$  with a detection limit of 52 nM.

**3.1.3. T-T mismatch-based electrochemical biosensors for  $\text{Hg}^{2+}$ .** Electrochemical biosensors based on redox-tagged, T-rich oligonucleotides have also been developed for  $\text{Hg}^{2+}$  analysis. By immobilizing ferrocene (Fc)-tagged, short, T-rich oligonucleotides onto a gold electrode

surface via self-assembly of the terminal thiol moiety, Jiang and coworkers (100) demonstrated an electrochemical biosensor for  $\text{Hg}^{2+}$  detection. In the presence of  $\text{Hg}^{2+}$ , the formation of a T- $\text{Hg}^{2+}$ -T base pair triggered a conformational change in the poly-T oligonucleotides from flexible single strands to relatively rigid duplex-like complexes, thus drawing the Fc tags away from the electrode and substantially decreasing the redox current. This sensor system allowed for the highly sensitive detection of  $\text{Hg}^{2+}$  with a detection limit of 0.5 nM. On the basis of a different design, Kim and coworkers (101) also modified an Fc-tagged, T-rich ssDNA on a gold electrode surface to detect  $\text{Hg}^{2+}$ . In their sensor system, however, the formation of T- $\text{Hg}^{2+}$ -T induced the T-rich sequence to fold, causing the Fc group to move closer to the electrode surface and to substantially increase the electrochemical signal. The two sensors discussed above depend on conformational changes to generate signals, and these techniques may suffer from a relatively small signal-to-background ratio because of the limited distance the redox tag can move from the electrode surface. Therefore, Chu and coworkers (102) developed an electrochemical  $\text{Hg}^{2+}$  sensor that was based on target-induced structure-switching DNA. A T-rich ssDNA strand was immobilized onto the gold electrode and hybridized with an Fc-tagged oligonucleotide, leading to a high redox current. In the presence of  $\text{Hg}^{2+}$ , the formation of T- $\text{Hg}^{2+}$ -T base pairs induced folding of the T-rich ssDNA strand into a hairpin structure, causing the release of the Fc-tagged oligonucleotide from the electrode surface and substantially decreasing the redox current.

AuNP-based amplifying strategies were also employed to construct T-T mismatch-based electrochemical biosensors for the amplified detection of  $\text{Hg}^{2+}$ . Zhang and coworkers (103) developed a T- $\text{Hg}^{2+}$ -T-based electrochemical  $\text{Hg}^{2+}$  biosensor that used AuNP-functionalized reporter DNA to amplify the signal, with methylene blue transducing the signal. The proposed sensor showed a detection limit of 0.5 nM for  $\text{Hg}^{2+}$ . Similarly, Li and coworkers (104) developed an electrochemical  $\text{Hg}^{2+}$  sensor with AuNPs as amplifiers and  $[\text{Ru}(\text{NH}_3)_6]^{3+}$  as an electrochemical signal transducer. Later, they immobilized a T-rich probe on a gold electrode surface to capture  $\text{Hg}^{2+}$  in aqueous solution, and the electrochemical reduction of surface-confined  $\text{Hg}^{2+}$  provided an electrochemical signal that allowed for the quantitative detection of  $\text{Hg}^{2+}$  (105). These investigators also improved the sensitivity of this  $\text{Hg}^{2+}$  sensor with AuNP-based signal amplification, leading to a detection limit of 0.5 nM.

Li and coworkers (106) also used electrochemical impedance spectroscopy to develop a T-T mismatch-based  $\text{Hg}^{2+}$  biosensor. A T-rich DNA probe was immobilized onto a gold electrode surface. In the presence of  $\text{Hg}^{2+}$ , the specific coordination between  $\text{Hg}^{2+}$  and the T bases caused linear ssDNA to form a hairpin. Partial DNA molecules were subsequently released from the surface of the electrode, and this process could be monitored by electrochemical impedance spectroscopy. Moreover, electrochemiluminescence was applied in designing  $\text{Hg}^{2+}$  biosensors based on T- $\text{Hg}^{2+}$ -T coordination chemistry. Chen and coworkers (107) designed an electrochemiluminescent biosensor for  $\text{Hg}^{2+}$  by attaching T-rich oligonucleotides to  $\text{Ru}(\text{bpy})_3^{2+}$ -doped silica nanoparticles for signal amplification.

**3.1.4. Other detection methods used to construct  $\text{Hg}^{2+}$  biosensors.** In addition to the detection methods discussed above, T- $\text{Hg}^{2+}$ -T coordination chemistry was used in conjunction with other methods to detect  $\text{Hg}^{2+}$ . Jiang and coworkers (108) immobilized T-rich ssDNA on 10-nm AuNPs to develop a resonance scattering probe for  $\text{Hg}^{2+}$  detection at concentrations as low as 0.7 nM. In the presence of  $\text{Hg}^{2+}$ , the formation of T- $\text{Hg}^{2+}$ -T base pairs induced AuNPs to aggregate, enhancing the intensity of resonance scattering at 540 nm. On the basis of a similar strategy, Huang and coworkers (109) reported a localized surface plasmon resonance light-scattering  $\text{Hg}^{2+}$  sensor with a detection limit of 1.0 nM. Dong and coworkers (110) also developed a T- $\text{Hg}^{2+}$ -T-based surface plasmon resonance sensor for  $\text{Hg}^{2+}$  using partially complementary

DNA-modified AuNPs to achieve signal amplification. Gao and coworkers (111) employed induced circular dichroism (ICD) to study the interactions of  $\text{Hg}^{2+}$  with the T-rich ssDNA wrapped around SWCNTs. These researchers developed a sensing system to detect  $\text{Hg}^{2+}$  at the nanomolar level by monitoring the  $\text{Hg}^{2+}$ -mediated ICD of T-rich DNA-SWCNTs (111). By taking advantage of the cooperative binding and catalytic properties of DNA-functionalized AuNPs and the selective binding of a T-T mismatch for  $\text{Hg}^{2+}$ , Lee & Mirkin (112) developed a chip-based scanometric method for the amplified detection of  $\text{Hg}^{2+}$  with a detection limit of 10 nM.

### 3.2. C-C Mismatch-Based Biosensors for $\text{Ag}^+$

Ono and coworkers (69) found that, similar to  $\text{Hg}^{2+}$ 's interactions with T-T mismatches,  $\text{Ag}^+$  can specifically bind to two cytosines (C) and can promote these C-C mismatches to form stable base pairs. A fluorescent biosensor for  $\text{Ag}^+$  was then developed on the basis of C- $\text{Ag}^+$ -C coordination chemistry (69). Fan and coworkers (113) developed a graphene oxide-based nanoprobe to detect  $\text{Ag}^+$  using a fluorophore-labeled C-rich oligonucleotide as a recognition unit and graphene oxide as an excellent quencher. More recently, Qu and coworkers (114) reported a reusable C-rich ssDNA-SWNT-based fluorescent  $\text{Ag}^+$  sensor with a detection limit of 1 nM. Taking advantage of the attractive optical properties of quantum dots, the Willner group (115) functionalized CdSe-ZnS quantum dots with T-rich and C-rich nucleic acids for the optically selective, multiplexed analysis of  $\text{Hg}^{2+}$  and  $\text{Ag}^+$ . On the basis of the target-induced conformational change of a poly-C DNA probe, Tseng and coworkers (116) developed a label-free fluorescent sensor for  $\text{Ag}^+$  using SYBR Green I as a fluorescent reporter.

Colorimetric biosensors that utilize an HRP-mimicking DNAzyme were also developed for  $\text{Ag}^+$ . The Dong group (117) used a C-rich quadruplex-duplex DNA structure as a DNAzyme switch for the colorimetric detection of  $\text{Ag}^+$  with a detection limit of 2.5 nM. On the basis of the  $\text{Ag}^+$ -mediated formation of the G-quadruplex-hemin DNAzyme, Kong and coworkers (118) developed a structure-switching colorimetric biosensor for the turn-on detection of  $\text{Ag}^+$  at concentrations as low as 20 nM.

## 4. METAL ION BIOSENSORS BASED ON G-QUADRUPLEXES

Guanine-rich segments of DNA can associate into four-stranded structures known as G-quadruplexes, which are characterized by stacked arrays of four guanine bases (**Figure 5a**). In addition to hydrogen-bonding forces, G-quadruplexes are selectively stabilized by metal ions such as  $\text{K}^+$  and  $\text{Pb}^{2+}$  (119, 120). The metal ion specificity of G-quadruplexes has been employed to develop biosensors for  $\text{K}^+$  and  $\text{Pb}^{2+}$ .

### 4.1. G-Quadruplex-Based Biosensors for $\text{K}^+$

$\text{K}^+$  plays an important role in biological systems, together with  $\text{Na}^+$ ,  $\text{Ca}^{2+}$ , and other metal ions. Therefore, the development of biosensors that can detect  $\text{K}^+$  is of great importance. The oligonucleotide contains four guanine-rich segments that offer a unique  $\text{K}^+$ -binding site, allowing folding to form a G-quadruplex. Moreover, G-quadruplex is highly specific for  $\text{K}^+$ , and therefore many groups have converted G-quadruplex into highly sensitive and selective fluorescent, colorimetric, and electrochemical sensors.

**4.1.1. G-quadruplex-based fluorescent biosensors for  $\text{K}^+$ .** Takenaka and coworkers (121) reported a G-quadruplex-based FRET probe for  $\text{K}^+$  ions (**Figure 5b**). The 21-mer human telomeric



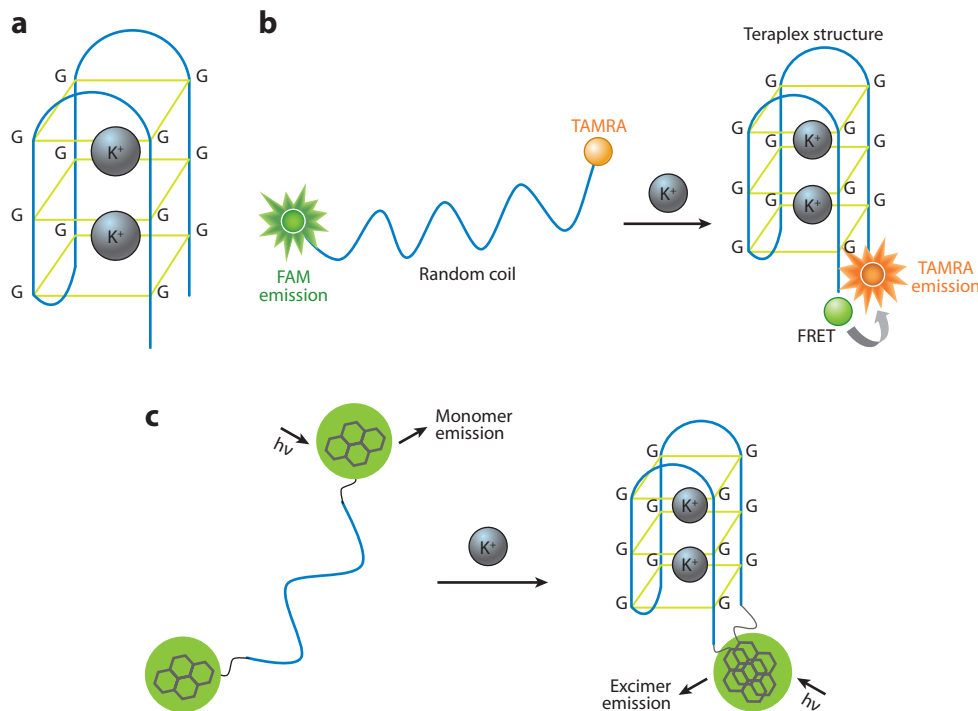


**Figure 5**

Strategies for designing G-quadruplex-based fluorescent  $K^+$  biosensors. (a) Structure of a G-quadruplex stabilized by  $K^+$ . (b) Schematic of a G-quadruplex-based fluorescence resonance energy transfer (FRET) probe for  $K^+$ . (c) Schematic of a G-quadruplex fluorescent probe for  $K^+$  based on pyrene monomer-excimer emission. Abbreviations: G, guanine base;  $h\nu$ , photon energy.

DNA was labeled with two fluorophores, 6-FAM and 6-TAMRA, at its two ends as the donor and the acceptor, respectively. In the presence of  $K^+$ , the probe formed a stable G-quadruplex with the two fluorophores in close enough proximity to allow for FRET. To improve the sensor's selectivity for  $K^+$  over  $Na^+$ , these investigators further developed a thrombin-binding aptamer that contains a G-quadruplex-based probe for the facile detection of  $K^+$  in the presence of excess  $Na^+$  (122). The 15-mer thrombin-binding aptamer was labeled with pyrene moieties at the two ends (**Figure 5c**). The binding of  $K^+$  induced a stable G-quadruplex to form; the two pyrene moieties were arranged face to face and emitted excimer fluorescence. In the absence of  $K^+$ , however, the random-coil structure of the probe gave only monomer emission. Takenaka and colleagues (123) further extended the thrombin-binding, aptamer-based probe using 6-FAM and 6-TAMRA as a FRET pair.

Taking advantage of the unique quenching property of AuNPs, the Fan group (124) coassembled dye-functionalized aptamers and their complementary sequences at the surfaces of AuNPs to develop a multicolor, fluorescent gold nanoprobe for multiplex detection. The addition of the target induced aptamer release, leading to an enhanced fluorescent signal. Such a multicolor fluorescent nanoprobe simultaneously detected  $K^+$ , adenosine, and cocaine with high selectivity.

Ho & Leclerc (125) designed a thrombin-binding, aptamer-based fluorescent biosensor for  $K^+$  using cation-conjugated polymers as fluorescent reporters. In the absence of  $K^+$ , the G-rich aptamer associated with the polymer to form a rigid double helix with quenched fluorescence.

The G-quadruplex that formed upon addition of  $K^+$  destabilized the interaction between the polymer and the aptamer, enhancing the fluorescent signal. Wang and coworkers (126) employed a different strategy to develop another  $K^+$  biosensor. G-rich DNA was labeled with fluorescein, and the electrostatic interaction of the DNA with the cation-conjugated polymer was weak because of its low charge density. The addition of  $K^+$  induced a compact G-quadruplex structure to form. Because the structure was compact, it had a higher charge density to interact more strongly with the cation-conjugated polymer, which allowed for more efficient energy transfer between the two species.

DNA-intercalating dyes were also used to design label-free fluorescent sensors for  $K^+$  on the basis of a G-quadruplex. Huang & Chang (127) employed OliGreen and an ATP-binding aptamer to construct a label-free fluorescent sensor for  $K^+$ .  $K^+$  decreased its fluorescent signal, and the sensor detected  $K^+$  at concentrations as low as 75 nM (127). Using a similar strategy, Kim and coworkers (128) used a molecular light-switch complex  $[Ru(phen)_2(dppz)^{2+}]$  and a  $K^+$ -binding aptamer to develop a label-free fluorescent sensor for  $K^+$ . Kim and coworkers (129) developed polydiacetylene liposome-based microarrays for the selective detection of  $K^+$ . G-rich ssDNA probes were densely covalently linked at the liposome surface and formed bulky quadruplexes once they were bound by  $K^+$ . The resulting bulky quadruplexes repelled one other, inducing a conformational change of the ene-yne backbone of the polydiacetylene liposome, and produced a red fluorescent emission.

**4.1.2. G-quadruplex-based colorimetric biosensors for  $K^+$ .** Beyond fluorescent biosensors, colorimetric G-quadruplex-based sensors were also developed for  $K^+$ . On the basis of the fact that AuNPs functionalized with folded aptamer structures are more stable toward salt-induced aggregation than are those tethered to unfolded aptamers, Li and coworkers (130) functionalized AuNPs with short thiolated aptamers to detect  $K^+$  and adenosine. Fan and coworkers (131) designed a G-quadruplex-based colorimetric biosensor for  $K^+$  with unmodified AuNPs on the basis of the protection effects of short ssDNA for AuNPs. In the presence of  $K^+$ , G-quadruplexes induced the desorbing of ssDNA from AuNPs, aggregating AuNPs and causing an observable color change. This sensor system detected  $\sim 1$  mM of  $K^+$ . Using a similar strategy, Jiang and coworkers (132) employed silver nanoparticles and resonance scattering spectroscopy to design a  $K^+$  biosensor.

Dong and coworkers (133) used an HRP-mimicking DNzyme as an amplifying color reporter to develop a colorimetric  $K^+$  biosensor. A G-rich ssDNA named AGRO100 was employed as a  $K^+$  probe. In the presence of  $K^+$ , even at the submicromolar level, the formation of a G-quadruplex structure significantly promoted the binding of AGRO100 to hemin, sharply increasing the DNzyme's activity. Through this colorimetric approach,  $K^+$  was easily detected at 0.1  $\mu$ M with good linearity and high selectivity. On the basis of a similar design, Wang and coworkers (134) also developed a colorimetric  $K^+$  biosensor using a  $K^+$ -dependent, G-quadruplex known as PS5.M as the sensing element and achieved a detection limit of 2  $\mu$ M.

**4.1.3. G-quadruplex-based electrochemical biosensors for  $K^+$ .** Radi & O'Sullivan (135) were the first to report a G-quadruplex-based electrochemical  $K^+$  biosensor with a detection limit of 15  $\mu$ M. A thiolated, Fc-tagged, G-rich  $K^+$  aptamer was immobilized onto a gold electrode via self-assembly of its terminal thiol. In the absence of  $K^+$ , the DNA unfolded, and the Fc group had a high probability of colliding with or even weakly binding to the electrode surface. In the presence of  $K^+$ , however, the formation of a G-quadruplex inhibited electron transfer between the Fc group and the electrode's surface, decreasing the electrochemical signal. Wu and coworkers (136) developed an electronic  $K^+$  nanoswitch based on the two-state transition between single-stranded random

coils and four-stranded intermolecular G-quadruplexes. Fc-labeled, G-rich DNA sequences were immobilized onto a gold electrode.  $K^+$  induced a four-stranded intermolecular G-quadruplex to form, moving the Fc groups away from the electrode surface and decreasing the electron-transfer efficiency from the Fc groups to the electrode surface.

#### 4.2. G-Quadruplex-Based Biosensors for $Pb^{2+}$

$Pb^{2+}$ -dependent, G-rich ssDNAs can be integrated into  $Pb^{2+}$  biosensors. Chang and coworkers (137) labeled a thrombin-binding aptamer with the donor FAM at one end and the quencher DABCYL at the other end to develop a fluorescent biosensor for the highly selective and sensitive detection of  $Pb^{2+}$  and  $Hg^{2+}$ . The thrombin-binding aptamer has a random-coil structure that changes into a G-quartet structure and a hairpin-like structure upon binding of  $Pb^{2+}$  and  $Hg^{2+}$ , respectively, moving the fluorophore closer to the quencher. As a result, the fluorescence intensity decreases, allowing for the selective detection of  $Pb^{2+}$  and  $Hg^{2+}$  ions at concentrations as low as 300 pM and 5.0 nM, respectively.

Wang and coworkers (138) found that  $Pb^{2+}$  induces a  $K^+$ -stabilized G-quadruplex DNAzyme to change its conformation and inhibits the DNAzyme's peroxidase-like activity. On the basis of this phenomenon, these investigators developed a  $Pb^{2+}$ -induced, allosteric G-quadruplex DNAzyme as a colorimetric and chemiluminescent  $Pb^{2+}$  biosensor. PS2.M, a common G-quadruplex DNAzyme, was chosen as the basis of a  $Pb^{2+}$  biosensor (139). In the presence of  $K^+$  and through the use of hemin as a cofactor, PS2.M's activity was enhanced, and PS2.M effectively catalyzed the  $H_2O_2$ -mediated oxidation of ABTS or luminol, producing either a color change or chemiluminescence. In the presence of  $Pb^{2+}$ ,  $K^+$ -stabilized PS2.M converted to a  $Pb^{2+}$ -stabilized structure, which was more stable but less active than the original structure, and led to a sharp decrease in the optical signal.

### 5. CONCLUSIONS AND OUTLOOK

We review here recent advances in the development and applications of DNAzyme-based biosensors for metal ions. Metal ions are of special interest because of their unique biological importance. DNAzymes provide a general platform for metal ion biosensors and have been customized for use in various signaling transduction strategies. The rapid development of the DNAzyme-based sensing field is undoubtedly a result of these properties, as well as other properties such as DNAzymes' facile and reproducible synthesis, easy and controllable modification to fulfill different sensing purposes, long-term stability in dry powder or aqueous solution, and ability to sustain reversible denaturation.

Optical platforms for metal ion sensing using DNAzymes conjugated to organic dyes or nanomaterials are currently much more common than electrochemical platforms. Many of these optical sensing systems show high sensitivity and specificity over competing metal ions. Nevertheless, many challenges remain. First, even though a number of DNAzymes have been selected to bind metal ions selectively, the structural features responsible for this selective binding remain to be elucidated (140–145). Furthermore, most of the DNAzyme-based biosensors currently available have been developed and tested in highly controlled buffer systems. Therefore, a future challenge is to apply these sensor systems to real-world medical diagnostics and environmental monitoring and in live specimens ranging from cells and tissue to whole organisms. More effort should be applied to improving the selectivity and sensitivity of these sensor systems in complex sample matrices. To accomplish in vivo sensing, the biological membrane penetrability as well as the intracellular stability of these sensor systems should be evaluated and improved as necessary. Moreover,

biological autofluorescence could cause serious interference for in vivo imaging, but materials with IR emissions or photon-upconverting materials could well eliminate such interference. In the near future, these two types of materials could attract an ever-increasing degree of interest and could become a major focus in the field of DNAzyme sensing.

## DISCLOSURE STATEMENT

The authors are not aware of any affiliations, memberships, funding, or financial holdings that might be perceived as affecting the objectivity of this review.

## ACKNOWLEDGMENTS

We thank Hannah Ihms for help with proofreading and the U.S. Department of Energy (DE-FG02-08ER64568), the National Institutes of Health (ES016865), the National Science Foundation (CTS-0120978 and DMI-0328162), and the National Natural Science Foundation of China (grant 20975034) for financial support.

## LITERATURE CITED

1. Nolan EM, Lippard SJ. 2008. Tools and tactics for the optical detection of mercuric ion. *Chem. Rev.* 108:3443–80
2. Thomas SW, Joly GD, Swager TM. 2007. Chemical sensors based on amplifying fluorescent conjugated polymers. *Chem. Rev.* 107:1339–86
3. Pazos E, Vazquez O, Mascarenas JL, Vazquez ME. 2009. Peptide-based fluorescent biosensors. *Chem. Soc. Rev.* 38:3348–59
4. Chen PR, He C. 2008. Selective recognition of metal ions by metalloregulatory proteins. *Curr. Opin. Chem. Biol.* 12:214–21
5. Verma N, Singh M. 2005. Biosensors for heavy metals. *Biometals* 18:121–29
6. Robertson DL, Joyce GF. 1990. Selection in vitro of an RNA enzyme that specifically cleaves single-stranded DNA. *Nature* 344:467–68
7. Lu Y, Liu J. 2006. Functional DNA nanotechnology: emerging applications of DNAzymes and aptamers. *Curr. Opin. Biotechnol.* 17:580–88
8. Navani NK, Li Y. 2006. Nucleic acid aptamers and enzymes as sensors. *Curr. Opin. Chem. Biol.* 10:272–81
9. Liu J, Brown AK, Meng X, Crokek DM, Istok JD, et al. 2007. A catalytic beacon sensor for uranium with parts-per-trillion sensitivity and million-fold selectivity. *Proc. Natl. Acad. Sci. USA* 104:2056–61
10. Storhoff JJ, Mirkin CA. 1999. Programmed materials synthesis with DNA. *Chem. Rev.* 99:1849–62
11. Breaker RR. 1997. DNA enzymes. *Nat. Biotechnol.* 15:427–31
12. Lu Y. 2002. New transition ion-dependent catalytic DNA and their applications as efficient RNA nuclease and as sensitive metal ion sensors. *Chem. Eur. J.* 8:4588–96
13. Breaker RR, Joyce GF. 1994. A DNA enzyme that cleaves RNA. *Chem. Biol.* 1:223–29
14. Li J, Lu Y. 2000. A highly sensitive and selective catalytic DNA biosensor for lead ions. *J. Am. Chem. Soc.* 122:10466–67
15. Carmi N, Shultz LA, Breaker RR. 1996. In vitro selection of self-cleaving DNAs. *Chem. Biol.* 3:1039–46
16. Wang W, Billen LP, Li Y. 2002. Sequence diversity, metal specificity, and catalytic proficiency of metal-dependent phosphorylating DNA enzymes. *Chem. Biol.* 9:507–17
17. Breaker RR, Joyce GF. 1995. A DNA enzyme with  $Mg^{2+}$ -dependent RNA phosphoesterase activity. *Chem. Biol.* 2:655–60
18. Faulhammer D, Famulok M. 1996. The  $Ca^{2+}$  ion as a cofactor for a novel RNA-cleaving deoxyribozyme. *Angew. Chem. Int. Ed.* 35:2837–41
19. Santoro SW, Joyce GF, Sakthivel K, Gramatikova S, Barbas CF. 2000. RNA cleavage by a DNA enzyme with extended chemical functionality. *J. Am. Chem. Soc.* 122:2433–39

20. Bruesehoff PJ, Li J, Augustine AJ, Lu Y. 2002. Improving metal ion specificity during in vitro selection of catalytic DNA. *Comb. Chem. High Throughput Screen.* 5:327–35
21. Mei SH, Liu Z, Brennan JD, Li Y. 2003. An efficient RNA-cleaving DNA enzyme that synchronizes catalysis with fluorescence signaling. *J. Am. Chem. Soc.* 125:412–20
22. Wang Y, Silverman SK. 2003. Deoxyribozymes that synthesize branched and lariat RNA. *J. Am. Chem. Soc.* 125:6880–81
23. Cruz RPG, Withers JB, Li Y. 2004. Dinucleotide junction cleavage versatility of 8-17 deoxyribozyme. *Chem. Biol.* 11:57–67
24. Hollenstein M, Hipolito C, Lam C, Dietrich D, Perrin DM. 2008. Highly selective DNazyme sensor for mercuric ions. *Angew. Chem. Int. Ed.* 47:4346–50
25. Tyagi S, Kramer FR. 1996. Molecular beacons: probes that fluoresce upon hybridization. *Nat. Biotechnol.* 14:303–8
26. Wang K, Tang Z, Yang CJ, Kim Y, Fang X, et al. 2009. Molecular engineering of DNA: molecular beacons. *Angew. Chem. Int. Ed.* 48:856–70
27. Santoro SW, Joyce GF. 1997. A general purpose RNA-cleaving DNA enzyme. *Proc. Natl. Acad. Sci. USA* 94:4262–66
28. Li J, Zheng W, Kwon AH, Lu Y. 2000. In vitro selection and characterization of a highly efficient Zn(II)-dependent RNA-cleaving deoxyribozyme. *Nucleic Acids Res.* 28:481–88
29. Schlosser K, Lam JCF, Li Y. 2006. Characterization of long RNA-cleaving deoxyribozymes with short catalytic cores: the effect of excess sequence elements on the outcome of in vitro selection. *Nucleic Acids Res.* 34:2445–54
30. Liu J, Lu Y. 2003. Improving fluorescent DNazyme biosensors by combining inter- and intramolecular quenchers. *Anal. Chem.* 75:6666–72
31. Liu J, Lu Y. 2007. A DNazyme catalytic beacon sensor for paramagnetic Cu<sup>2+</sup> ions in aqueous solution with high sensitivity and selectivity. *J. Am. Chem. Soc.* 129:9838–39
32. Mei SHJ, Liu Z, Brennan JD, Li Y. 2003. An efficient RNA-cleaving DNA enzyme that synchronizes catalysis with fluorescence signaling. *J. Am. Chem. Soc.* 125:412–20
33. Liu Z, Mei SHJ, Brennan JD, Li Y. 2003. Assemblage of signaling DNA enzymes with intriguing metal-ion specificities and pH dependences. *J. Am. Chem. Soc.* 125:7539–45
34. Chiuman W, Li Y. 2007. Efficient signaling platforms built from a small catalytic DNA and doubly labeled fluorogenic substrates. *Nucleic Acids Res.* 35:401–5
35. Shen Y, Mackey G, Rupcich N, Gloster D, Chiuman W, et al. 2007. Entrapment of fluorescence signaling DNA enzymes in sol-gel-derived materials for metal ion sensing. *Anal. Chem.* 79:3494–503
36. Nagraj N, Liu J, Sterling S, Wu J, Lu Y. 2009. DNazyme catalytic beacon sensors that resist temperature-dependent variations. *Chem. Commun.* 2009:4103–5
37. Lan T, Furuya K, Lu Y. 2010. A highly selective lead sensor based on a classic lead DNazyme. *Chem. Commun.* 46:3896–98
38. Wang H, Kim Y, Liu H, Zhu Z, Bamrungsap S, et al. 2009. Engineering a unimolecular DNA-catalytic probe for single lead ion monitoring. *J. Am. Chem. Soc.* 131:8221–26
39. Zhang XB, Wang Z, Xing H, Xiang Y, Lu Y. 2010. Catalytic and molecular beacons for amplified detection of metal ions and organic molecules with high sensitivity. *Anal. Chem.* 82:5005–11
40. Xiang Y, Tong A, Lu Y. 2009. Abasic site-containing DNazyme and aptamer for label-free fluorescent detection of Pb<sup>2+</sup> and adenosine with high sensitivity, selectivity, and tunable dynamic range. *J. Am. Chem. Soc.* 131:15352–57
41. Xiang Y, Wang Z, Xing H, Wong NY, Lu Y. 2010. Label-free fluorescent functional DNA sensors using unmodified DNA: a vacant site approach. *Anal. Chem.* 82:4122–29
42. Swearingen CB, Wernette DP, Cropek DM, Lu Y, Sweedler JV, et al. 2005. Immobilization of a catalytic DNA molecular beacon on Au for Pb<sup>2+</sup> detection. *Anal. Chem.* 77:442–48
43. Wernette DP, Swearingen CB, Cropek DM, Lu Y, Sweedler JV, et al. 2006. Incorporation of a DNazyme into Au-coated nanocapillary array membranes with an internal standard for Pb<sup>2+</sup> sensing. *Analyst* 131:41–47
44. Wernette DP, Mead C, Bohn PW, Lu Y. 2007. Surface immobilization of catalytic beacons based on ratiometric fluorescent DNazyme sensors: a systematic study. *Langmuir* 23:9513–21

45. Yim TJ, Liu J, Lu Y, Kane RS, Dordick JS. 2005. Highly active and stable DNAzyme-carbon nanotube hybrids. *J. Am. Chem. Soc.* 127:12200–1
46. McDonald JC, Whitesides GM. 2002. Poly(dimethylsiloxane) as a material for fabricating microfluidic devices. *Acc. Chem. Res.* 35:491–99
47. Zhang C, Xing D. 2010. Single-molecule DNA amplification and analysis using microfluidics. *Chem. Rev.* 110:4910–47
48. Shaikh KA, Ryu KS, Goluch ED, Nam JM, Liu J, et al. 2005. A modular microfluidic architecture for integrated biochemical analysis. *Proc. Natl. Acad. Sci. USA* 102:9745–50
49. Chang IH, Tulock JJ, Liu J, Kim WS, Cannon DM Jr, et al. 2005. Miniaturized lead sensor based on lead-specific DNAzyme in a nanocapillary interconnected microfluidic device. *Environ. Sci. Technol.* 39:3756–61
50. Dalavoy TS, Wernette DP, Gong M, Sweedler JV, Lu Y, et al. 2008. Immobilization of DNAzyme catalytic beacons on PMMA for  $Pb^{2+}$  detection. *Lab. Chip* 8:786–93
51. Daniel MC, Astruc D. 2004. Gold nanoparticles: assembly, supramolecular chemistry, quantum-size-related properties, and applications toward biology, catalysis, and nanotechnology. *Chem. Rev.* 104:293–46
52. Liu J, Lu Y. 2003. A colorimetric lead biosensor using DNAzyme-directed assembly of gold nanoparticles. *J. Am. Chem. Soc.* 125:6642–43
53. Liu J, Lu Y. 2004. Accelerated color change of gold nanoparticles assembled by DNAzymes for simple and fast colorimetric  $Pb^{2+}$  detection. *J. Am. Chem. Soc.* 126:12298–305
54. Liu J, Lu Y. 2005. Stimuli-responsive disassembly of nanoparticle aggregates for light-up colorimetric sensing. *J. Am. Chem. Soc.* 127:12677–83
55. Liu J, Lu Y. 2006. Design of asymmetric DNAzymes for dynamic control of nanoparticle aggregation states in response to chemical stimuli. *Org. Biomol. Chem.* 4:3435–41
56. Lee JH, Wang Z, Liu J, Lu Y. 2008. Highly sensitive and selective colorimetric sensors for uranyl ( $UO_2^{2+}$ ): development and comparison of labeled and label-free DNAzyme-gold nanoparticle systems. *J. Am. Chem. Soc.* 130:14217–26
57. Liu J, Lu Y. 2007. Colorimetric  $Cu^{2+}$  detection with a ligation DNAzyme and nanoparticles. *Chem. Commun.* 46:4872–74
58. Zhao WA, Lam JCF, Chiuman W, Brook MA, Li YF. 2008. Enzymatic cleavage of nucleic acids on gold nanoparticles: a generic platform for facile colorimetric biosensors. *Small* 4:810–16
59. Wang ZD, Lee JH, Lu Y. 2008. Label-free colorimetric detection of lead ions with a nanomolar detection limit and tunable dynamic range by using gold nanoparticles and DNAzyme. *Adv. Mater.* 20:3263–67
60. Wei H, Li B, Li J, Dong S, Wang E. 2008. DNAzyme-based colorimetric sensing of  $Pb^{2+}$  using unmodified gold nanoparticle probes. *Nanotechnology* 19:095501
61. Mazumdar D, Liu J, Lu G, Zhou J, Lu Y. 2010. Easy-to-use dipstick tests for detection of lead in paints using non-cross-linked gold nanoparticle-DNAzyme conjugates. *Chem. Commun.* 46:1416–18
62. Elbaz J, Shlyahovsky B, Willner I. 2008. A DNAzyme cascade for the amplified detection of  $Pb^{2+}$  ions or L-histidine. *Chem. Commun.* 2008:1569–71
63. Moshe M, Elbaz J, Willner I. 2009. Sensing of  $UO_2^{2+}$  and design of logic gates by the application of supramolecular constructs of ion-dependent DNAzymes. *Nano Lett.* 9:1196–200
64. Yin BC, Ye BC, Tan W, Wang H, Xie CC. 2009. An allosteric dual-DNAzyme unimolecular probe for colorimetric detection of  $Cu^{2+}$ . *J. Am. Chem. Soc.* 131:14624–25
65. Xiao Y, Rowe AA, Plaxco KW. 2007. Electrochemical detection of parts-per-billion lead via an electrode-bound DNAzyme assembly. *J. Am. Chem. Soc.* 129:262–63
66. Shen L, Chen Z, Li Y, He S, Xie S, et al. 2008. Electrochemical DNAzyme sensor for lead based on amplification of DNA–Au bio-bar codes. *Anal. Chem.* 80:6323–28
67. Yang X, Xu J, Tang X, Liu H, Tian D. 2010. A novel electrochemical DNAzyme sensor for the amplified detection of  $Pb^{2+}$  ions. *Chem. Commun.* 46:3107–9
68. Ono A, Togashi H. 2004. Highly selective oligonucleotide-based sensor for mercury in aqueous solutions. *Angew. Chem. Int. Ed.* 43:4300–2
69. Ono A, Cao S, Togashi H, Tashiro M, Fujimoto T, et al. 2008. Specific interactions between silver(I) ions and cytosine-cytosine pairs in DNA duplexes. *Chem. Commun.* 2008:4825–27



70. Miyake Y, Togashi H, Tashiro M, Yamaguchi H, Oda S, et al. 2006. Mercury-mediated formation of thymine-Hg<sup>2+</sup>-thymine base pairs in DNA duplexes. *J. Am. Chem. Soc.* 128:2172–73
71. Tanaka Y, Oda S, Yamaguchi H, Kondo Y, Kojima C, et al. 2007. <sup>15</sup>N-<sup>15</sup>N J-coupling across Hg<sup>2+</sup>: direct observation of Hg<sup>2+</sup>-mediated T-T base pairs in a DNA duplex. *J. Am. Chem. Soc.* 129:244–45
72. Guo L, Hu H, Sun R, Chen G. 2009. Highly sensitive fluorescent sensor for mercury ion based on photoinduced charge transfer between fluorophore and stacked T-Hg<sup>2+</sup>-T base pairs. *Talanta* 79:775–79
73. Liu J, Lu Y. 2007. Rational design of “turn-on” allosteric DNzyme catalytic beacons for aqueous mercury ions with ultrahigh sensitivity and selectivity. *Angew. Chem. Int. Ed.* 46:7587–90
74. Wang Z, Lee JH, Lu Y. 2008. Highly sensitive “turn-on” fluorescent sensor for Hg<sup>2+</sup> in aqueous solution based on structure-switching DNA. *Chem. Commun.* 2008:6005–7
75. Wang H, Wang Y, Jin J, Yang R. 2008. Gold nanoparticle-based colorimetric and “turn-on” fluorescent probe for mercury ions in aqueous solution. *Anal. Chem.* 80:9021–28
76. Zhang L, Li T, Li B, Li J, Wang E. 2010. Carbon nanotube-DNA hybrid fluorescent sensor for sensitive and selective detection of mercury ion. *Chem. Commun.* 46:1476–78
77. Ye BC, Yin BC. 2008. Highly sensitive detection of mercury ions by fluorescence polarization enhanced by gold nanoparticles. *Angew. Chem. Int. Ed.* 47:8386–89
78. Chiang CK, Huang CC, Liu CW, Chang HT. 2008. Oligonucleotide-based fluorescence probe for sensitive and selective detection of mercury in aqueous solution. *Anal. Chem.* 80:3716–21
79. Wang J, Liu B. 2008. Highly sensitive and selective detection of Hg<sup>2+</sup> in aqueous solution with mercury-specific DNA and SYBR Green I. *Chem. Commun.* 2008:4759–61
80. Liu B. 2008. Highly sensitive oligonucleotide-based fluorometric detection of mercury in aqueous media. *Biosens. Bioelectron.* 24:762–66
81. Zhu X, Zhou X, Xing D. 2010. Ultrasensitive and selective detection of mercury(II) in aqueous solution by polymerase assisted fluorescence amplification. *Biosens. Bioelectron.* 26:2666–69
82. Liu CW, Huang CC, Chang HT. 2008. Control over surface DNA density on gold nanoparticles allows selective and sensitive detection of mercury. *Langmuir* 24:8346–50
83. Kumar M, Zhang P. 2010. Highly sensitive and selective label-free optical detection of mercuric ions using photon upconverting nanoparticles. *Biosens. Bioelectron.* 25:2431–35
84. Zhang X, Li Y, Su H, Zhang S. 2010. Highly sensitive and selective detection of Hg<sup>2+</sup> using mismatched DNA and a molecular light switch complex in aqueous solution. *Biosens. Bioelectron.* 25:1338–43
85. Liu X, Tang Y, Wang L, Zhang J, Song S, et al. 2007. Optical detection of mercury in aqueous solutions by using conjugated polymers and label-free oligonucleotides. *Adv. Mater.* 19:1471–74
86. Ren X, Xu QH. 2009. Highly sensitive and selective detection of mercury ions by using oligonucleotides, DNA intercalators, and conjugated polymers. *Langmuir* 25:29–31
87. Wang Y, Liu B. 2009. Amplified fluorescence turn-on assay for mercury detection and quantification based on conjugated polymer and silica nanoparticles. *Macromol. Rapid Commun.* 30:498–503
88. Lee JS, Han MS, Mirkin CA. 2007. Colorimetric detection of mercuric ion in aqueous media using DNA-functionalized gold nanoparticles. *Angew. Chem. Int. Ed.* 46:4093–96
89. Xue X, Wang F, Liu X. 2008. One-step, room temperature, colorimetric detection of mercury using DNA/nanoparticle conjugates. *J. Am. Chem. Soc.* 130:3244–45
90. He S, Li D, Zhu C, Song S, Wang L, et al. 2008. Design of a gold nanoprobe for rapid and portable mercury detection with the naked eye. *Chem. Commun.* 2008:4885–87
91. Li D, Wieckowska A, Willner I. 2008. Optical analysis of Hg<sup>2+</sup> ions by oligonucleotide-gold-nanoparticle hybrids and DNA-based machines. *Angew. Chem. Int. Ed.* 47:3927–31
92. Xu X, Wang J, Jiao K, Yang X. 2009. Colorimetric detection of mercury ion based on DNA oligonucleotides and unmodified gold nanoparticles sensing system with a tunable detection range. *Biosens. Bioelectron.* 24:3153–58
93. Li L, Li B, Qi Y, Jin Y. 2009. Label-free aptamer-based colorimetric detection of mercury ions in aqueous media using unmodified gold nanoparticles as colorimetric probe. *Anal. Bioanal. Chem.* 393:2051–57
94. Yu CJ, Cheng TL, Tseng WL. 2009. Effects of Mn<sup>2+</sup> on oligonucleotide-gold nanoparticle hybrids for colorimetric sensing of Hg<sup>2+</sup>: improving colorimetric sensitivity and accelerating color change. *Biosens. Bioelectron.* 25:204–10

95. Li T, Dong S, Wang E. 2009. Label-free colorimetric detection of aqueous mercury ion using  $\text{Hg}^{2+}$ -modulated G-quadruplex-based DNazymes. *Anal. Chem.* 81:2144–49
96. Li T, Li B, Wang E, Dong S. 2009. G-quadruplex-based DNzyme for sensitive mercury detection with the naked eye. *Chem. Commun.* 2009:3551–53
97. Li J, Yao J, Zhong W. 2009. Membrane blotting for rapid detection of mercury in water. *Chem. Commun.* 2009:4962–64
98. Lu N, Shao C, Deng Z. 2009. Colorimetric  $\text{Hg}^{2+}$  detection with a label-free and fully DNA-structured sensor assembly incorporating G-quadruplex halves. *Analyst* 134:1822–25
99. Kong DM, Wu J, Wang N, Yang W, Shen HX. 2009. Peroxidase activity-structure relationship of the intermolecular four-stranded G-quadruplex-hemin complexes and their application in  $\text{Hg}^{2+}$  ion detection. *Talanta* 80:459–65
100. Liu SJ, Nie HG, Jiang JH, Shen GL, Yu RQ. 2009. Electrochemical sensor for mercury based on conformational switch mediated by inter-strand cooperative coordination. *Anal. Chem.* 81:5724–30
101. Han D, Kim Y-R, Oh JW, Kim TH, Mahajan RK, et al. 2009. A regenerative electrochemical sensor based on oligonucleotide for the selective determination of mercury. *Analyst* 134:1857–62
102. Wu D, Zhang Q, Chu X, Wang H, Shen G, et al. 2010. Ultrasensitive electrochemical sensor for mercury based on target-induced structure-switching DNA. *Biosens. Bioelectron.* 25:1025–31
103. Kong RM, Zhang XB, Zhang LL, Jin XY, Huan SY, et al. 2009. An ultrasensitive electrochemical “turn-on” label-free biosensor for  $\text{Hg}^{2+}$  with AuNP-functionalized reporter DNA as a signal amplifier. *Chem. Commun.* 2009:5633–35
104. Miao P, Liu L, Li Y, Li G. 2009. A novel electrochemical method to detect mercury ions. *Electrochem. Commun.* 11:1904–7
105. Zhu Z, Su Y, Li J, Li D, Zhang J, et al. 2009. Highly sensitive electrochemical sensor for mercury ions by using a mercury-specific oligonucleotide probe and gold nanoparticle-based amplification. *Anal. Chem.* 81:7660–66
106. Cao RG, Zhu B, Li J, Xu D. 2009. Oligonucleotides-based biosensors with high sensitivity and selectivity for mercury using electrochemical impedance spectroscopy. *Electrochem. Commun.* 11:1815–18
107. Zhu X, Chen L, Lin Z, Qiu B, Chen G. 2010. A highly sensitive and selective signal-on electrochemiluminescent biosensor for mercury. *Chem. Commun.* 46:3149–52
108. Jiang Z, Fan Y, Chen M, Liang A, Liao X, et al. 2009. Resonance scattering spectral detection of trace  $\text{Hg}^{2+}$  using aptamer-modified nanogold as probe and nanocatalyst. *Anal. Chem.* 81:5439–45
109. Liu Z, Li Y, Ling J, Huang C. 2009. A localized surface plasmon resonance light-scattering assay of mercury(II) on the basis of  $\text{Hg}^{2+}$ -DNA complex induced aggregation of gold nanoparticles. *Environ. Sci. Technol.* 43:5022–27
110. Wang L, Li T, Du Y, Chen C, Li B, et al. 2010. Au NPs-enhanced surface plasmon resonance for sensitive detection of mercury ions. *Biosens. Bioelectron.* 25:2622–26
111. Gao X, Xing G, Yang Y, Shi X, Liu R, et al. 2008. Detection of trace  $\text{Hg}^{2+}$  via induced circular dichroism of DNA wrapped around single-walled carbon nanotubes. *J. Am. Chem. Soc.* 130:9190–91
112. Lee JS, Mirkin CA. 2008. Chip-based scanometric detection of mercuric ion using DNA-functionalized gold nanoparticles. *Anal. Chem.* 80:6805–8
113. Wen Y, Xing F, He S, Song S, Wang L, et al. 2010. A graphene-based fluorescent nanoprobe for silver(I) ions detection by using graphene oxide and a silver-specific oligonucleotide. *Chem. Commun.* 46:2596–98
114. Zhao C, Qu K, Song Y, Xu C, Ren J, et al. 2010. A reusable DNA single-walled carbon-nanotube-based fluorescent sensor for highly sensitive and selective detection of  $\text{Ag}^{+}$  and cysteine in aqueous solutions. *Chem. Eur. J.* 16:8147–54
115. Freeman R, Finder T, Willner I. 2009. Multiplexed analysis of  $\text{Hg}^{2+}$  and  $\text{Ag}^{+}$  ions by nucleic acid functionalized CdSe/ZnS quantum dots and their use for logic gate operations. *Angew. Chem. Int. Ed.* 48:7818–21
116. Lina YH, Tseng WL. 2009. Highly sensitive and selective detection of silver ions and silver nanoparticles in aqueous solution using an oligonucleotide-based fluorogenic probe. *Chem. Commun.* 2009:6619–21
117. Li T, Shi L, Wang E, Dong S. 2009. Silver-ion-mediated DNzyme switch for the ultrasensitive and selective colorimetric detection of aqueous  $\text{Ag}^{+}$  and cysteine. *Chem. Eur. J.* 15:3347–50

118. Kong DM, Cai LL, Shen HX. 2010. Quantitative detection of Ag<sup>+</sup> and cysteine using G-quadruplex-hemin DNazymes. *Analyst* 135:1253–58
119. Guschlbauer W, Chantot JF, Thiele D. 1990. Four-stranded nucleic acid structures 25 years later: from guanosine gels to telomere DNA. *Biomol. Struct. Dyn.* 8:491–511
120. Smirnov I, Shafer RH. 2000. Lead is unusually effective in sequence-specific folding of DNA. *J. Mol. Biol.* 296:1–5
121. Ueyama H, Takagi M, Takenaka S. 2002. A novel potassium sensing in aqueous media with a synthetic oligonucleotide derivative. Fluorescence resonance energy transfer associated with guanine quartet-potassium ion complex formation. *J. Am. Chem. Soc.* 124:14286–87
122. Nagatoishi S, Nojima T, Juskowiak B, Takenaka S. 2005. A pyrene-labeled G-quadruplex oligonucleotide as a fluorescent probe for potassium ion detection in biological applications. *Angew. Chem. Int. Ed.* 44:5067–70
123. Nagatoishi S, Nojima T, Galezowska E, Juskowiak B, Takenaka S. 2006. G quadruplex-based FRET probes with the thrombin-binding aptamer (TBA) sequence designed for the efficient fluorometric detection of the potassium ion. *ChemBioChem* 7:1730–37
124. Zhang J, Wang L, Zhang H, Boey F, Song S, et al. 2009. Aptamer-based multicolor fluorescent gold nanoprobe for multiplex detection in homogeneous solution. *Small* 6:201–4
125. Ho HA, Leclerc M. 2004. Optical sensors based on hybrid aptamer/conjugated polymer complexes. *J. Am. Chem. Soc.* 126:1384–87
126. He F, Tang Y, Wang S, Li Y, Zhu D. 2005. Fluorescent amplifying recognition for DNA G-quadruplex folding with a cationic conjugated polymer: a platform for homogeneous potassium detection. *J. Am. Chem. Soc.* 127:12343–46
127. Huang CC, Chang H-T. 2008. Aptamer-based fluorescence sensor for rapid detection of potassium ions in urine. *Chem. Commun.* 2008:1461–63
128. Choi MS, Yoon M, Baeg JO, Kim J. 2009. Label-free dual assay of DNA sequences and potassium ions using an aptamer probe and a molecular light switch complex. *Chem. Commun.* 2009:7419–21
129. Lee J, Kim H-J, Kim J. 2008. Polydiacetylene liposome arrays for selective potassium detection. *J. Am. Chem. Soc.* 130:5010–11
130. Zhao W, Chiuman W, Lam JCF, McManus SA, Chen W, et al. 2008. DNA aptamer folding on gold nanoparticles: from colloid chemistry to biosensors. *J. Am. Chem. Soc.* 130:3610–18
131. Wang L, Liu X, Hu X, Song S, Fan C. 2006. Unmodified gold nanoparticles as a colorimetric probe for potassium DNA aptamers. *Chem. Commun.* 2006:3780–82
132. Cai W, Fan Y, Jiang Z, Yao J. 2010. A highly sensitive and selective resonance scattering spectral assay for potassium ion based on aptamer and nanosilver aggregation reactions. *Talanta* 81:1810–15
133. Li T, Wang E, Dong S. 2009. G-quadruplex-based DNzyme as a sensing platform for ultrasensitive colorimetric potassium detection. *Chem. Commun.* 2009:580–82
134. Yang X, Li T, Li B, Wang E. 2010. Potassium-sensitive G-quadruplex DNA for sensitive visible potassium detection. *Analyst* 135:71–75
135. Radi AE, O'Sullivan CK. 2006. Aptamer conformational switch as sensitive electrochemical biosensor for potassium ion recognition. *Chem. Commun.* 2006:3432–34
136. Wu ZS, Chen CR, Shen GL, Yu RQ. 2008. Reversible electronic nanoswitch based on DNA G-quadruplex conformation: a platform for single-step, reagentless potassium detection. *Biomaterials* 29:2689–96
137. Liu CW, Huang CC, Chang H-T. 2009. Highly selective DNA-based sensor for lead and mercury ions. *Anal. Chem.* 81:2383–87
138. Li T, Wang E, Dong S. 2009. Potassium-lead-switched G-quadruplexes: a new class of DNA logic gates. *J. Am. Chem. Soc.* 131:15082–83
139. Li T, Wang E, Dong S. 2010. Lead-induced allosteric G-quadruplex DNzyme as a colorimetric and chemiluminescence sensor for highly sensitive and selective Pb<sup>2+</sup> detection. *Anal. Chem.* 82:1515–20
140. Liu J, Lu Y. 2002. FRET study of a trifluorophore-labeled DNzyme. *J. Am. Chem. Soc.* 124:15208–16
141. Kim HK, Liu J, Li J, Nagraj N, Li M, et al. 2007. Metal-dependent global folding and activity of the 8-17 DNzyme studied by fluorescence resonance energy transfer. *J. Am. Chem. Soc.* 129:6896–902

142. Kim HK, Rasnik I, Liu J, Ha T, Lu Y. 2007. Dissecting metal ion dependent folding and catalysis of a single DNzyme. *Nature Chem. Biol.* 3:763–68
143. Kim HK, Li J, Nagraj N, Lu Y. 2008. Probing metal binding in the 8-17 DNzyme via Tb<sup>III</sup> luminescence spectroscopy. *Chem. Eur. J.* 14:8696–703
144. Brown AK, Liu J, He Y, Lu Y. 2009. Biochemical characterization of a uranyl ion-specific DNzyme. *ChemBioChem* 10:486–92
145. Mazumdar D, Nagraj N, Kim HK, Meng X, Brown AK, et al. Activity, folding and Z-DNA formation of the 8-17 DNzyme in the presence of monovalent ions. *J. Am. Chem. Soc.* 131:5506–15



# Contents

A Century of Progress in Molecular Mass Spectrometry <i>Fred W. McLafferty</i> .....	1
Modeling the Structure and Composition of Nanoparticles by Extended X-Ray Absorption Fine-Structure Spectroscopy <i>Anatoly I. Frenkel, Aaron Yevick, Chana Cooper, and Relja Vasic</i> .....	23
Adsorption Microcalorimetry: Recent Advances in Instrumentation and Application <i>Matthew C. Crowe and Charles T. Campbell</i> .....	41
Microfluidics Using Spatially Defined Arrays of Droplets in One, Two, and Three Dimensions <i>Rebecca R. Pompano, Weishan Liu, Wenbin Du, and Rustem F. Ismagilov</i> .....	59
Soft Landing of Complex Molecules on Surfaces <i>Grant E. Johnson, Qichi Hu, and Julia Laskin</i> .....	83
Metal Ion Sensors Based on DNazymes and Related DNA Molecules <i>Xiao-Bing Zhang, Rong-Mei Kong, and Yi Lu</i> .....	105
Shell-Isolated Nanoparticle-Enhanced Raman Spectroscopy: Expanding the Versatility of Surface-Enhanced Raman Scattering <i>Jason R. Anema, Jian-Feng Li, Zhi-Lin Yang, Bin Ren, and Zhong-Qun Tian</i> .....	129
High-Throughput Biosensors for Multiplexed Food-Borne Pathogen Detection <i>Andrew G. Gebring and Shu-I Tu</i> .....	151
Analytical Chemistry in Molecular Electronics <i>Adam Johan Berggren and Richard L. McCreery</i> .....	173
Monolithic Phases for Ion Chromatography <i>Anna Nordborg, Emily F. Hilder, and Paul R. Haddad</i> .....	197
Small-Volume Nuclear Magnetic Resonance Spectroscopy <i>Raluca M. Fratila and Aldrik H. Velders</i> .....	227

The Use of Magnetic Nanoparticles in Analytical Chemistry <i>Jacob S. Beveridge, Jason R. Stephens, and Mary Elizabeth Williams</i> .....	251
Controlling Mass Transport in Microfluidic Devices <i>Jason S. Kuo and Daniel T. Chiu</i> .....	275
Bioluminescence and Its Impact on Bioanalysis <i>Daniel Scott, Emre Dikici, Mark Ensor, and Sylvia Daunert</i> .....	297
Transport and Sensing in Nanofluidic Devices <i>Kaimeng Zhou, John M. Perry, and Stephen C. Jacobson</i> .....	321
Vibrational Spectroscopy of Biomembranes <i>Zachary D. Schultz and Ira W. Levin</i> .....	343
New Technologies for Glycomic Analysis: Toward a Systematic Understanding of the Glycome <i>John F. Rakus and Lara K. Mahal</i> .....	367
The Asphaltenes <i>Oliver C. Mullins</i> .....	393
Second-Order Nonlinear Optical Imaging of Chiral Crystals <i>David J. Kissick, Debbie Wanapun, and Garth J. Simpson</i> .....	419
Heparin Characterization: Challenges and Solutions <i>Christopher J. Jones, Szabolcs Beni, John F.K. Limtiaco, Derek J. Langeslay, and Cynthia K. Larive</i> .....	439
 <b>Indexes</b>	
Cumulative Index of Contributing Authors, Volumes 1–4 .....	467
Cumulative Index of Chapter Titles, Volumes 1–4 .....	470

## Errata

An online log of corrections to the *Annual Review of Analytical Chemistry* articles may be found at <http://arjournals.annualreviews.org/errata/anchem>